Approved for public release;
Distribution unlimited

ENVPREDRSCHFAC
Technical Paper No. 14-74

MESOSCALE FEEDBACK FROM THE OCEAN TO THE ATMOSPHERE IN COASTAL AND OCEANIC FRONTAL REGIONS

by
T. LAEVASTU
and
CAPT. GLENN D. HAMILTON, USN

SEPTEMBER 1974

ENVIRONMENTAL PREDICTION RESEARCH FACILITY
NAVAL POSTGRADUATE SCHOOL
MONTEREY, CALIFORNIA 93940

UNCLASSIFIED

SECURITY CLASSIFICATION OF THIS PAGE *(When Data Entered)*

REPORT DOCUMENTATION PAGE

READ INSTRUCTIONS BEFORE COMPLETING FORM

1. REPORT NUMBER: ENVPREDRSCHFAC Technical Paper No. 14-74
2. GOVT ACCESSION NO.:
3. RECIPIENT'S CATALOG NUMBER:

4. TITLE *(and Subtitle)*: Mesoscale Feedback from the Ocean to the Atmosphere in Coastal and Oceanic Frontal Regions

5. TYPE OF REPORT & PERIOD COVERED:

6. PERFORMING ORG. REPORT NUMBER:

7. AUTHOR(s): T. Laevastu and G. D. Hamilton

8. CONTRACT OR GRANT NUMBER(s):

9. PERFORMING ORGANIZATION NAME AND ADDRESS:
Environmental Prediction Research Facility
Naval Postgraduate School
Monterey, CA 93940

10. PROGRAM ELEMENT, PROJECT, TASK AREA & WORK UNIT NUMBERS:
PE:62759N PN:52551
TA: WF52-551-713
EPRF WU No. 054:2-3

11. CONTROLLING OFFICE NAME AND ADDRESS:
Naval Air Systems Command
Department of the Navy
Washington, D.C. 20361

12. REPORT DATE: September 1974

13. NUMBER OF PAGES: 46

14. MONITORING AGENCY NAME & ADDRESS *(if different from Controlling Office)*:

15. SECURITY CLASS. *(of this report)*: UNCLASSIFIED

15a. DECLASSIFICATION/DOWNGRADING SCHEDULE:

16. DISTRIBUTION STATEMENT *(of this Report)*:
Approved for public release; Distribution unlimited.

17. DISTRIBUTION STATEMENT *(of the abstract entered in Block 20, if different from Report)*:

18. SUPPLEMENTARY NOTES:

19. KEY WORDS *(Continue on reverse side if necessary and identify by block number)*:
Air-sea interaction
Coastal influence
Oceanic frontal effects
Numerical modeling
Heat and moisture transfer

20. ABSTRACT *(Continue on reverse side if necessary and identify by block number)*:

The most intensive interaction between the sea and the atmosphere occurs in the areas of strong thermal gradients such as coastal regions and oceanic frontal areas. This interaction is essentially a mesoscale process. A brief review of some feedback models is presented and the essential factors in the feedback processes are outlined. The most important aspect in

DD FORM 1 JAN 73 1473 EDITION OF 1 NOV 65 IS OBSOLETE
S/N 0102-014-6601 |

UNCLASSIFIED

SECURITY CLASSIFICATION OF THIS PAGE *(When Data Entered)*

20. (continued)

mesoscale feedback seems to be the speed of response of the surface air properties to the corresponding properties of the sea surface. Theoretical formulations to account for this response are presented. The response time is found to be about 5 hours.

The verification of the theory is carried out with special measurements and recordings off the coast of California as well as with ship observations in the Labrador Current-Gulf Stream boundary area near Newfoundland. Off California and elsewhere along the continents, the "range of coastal influence" can be determined from the variation of the differences between the properties of the sea and air. The range of coastal influence is also demarcated with a coastal front 10 to 50 n mi from the coast. Often there is a marked change of surface winds at the coastal fronts. In the Labrador Current-Gulf Stream frontal area, some of the frontal influence on surface winds can be traced even with relatively sparce ship observations. Finally, some suggestions are made for more accurate accounting of the sea-air interactions in numerical models.

CONTENTS

LIST OF FIGURES

LIST OF FIGURES (continued)

LIST OF FIGURES (continued)

1. INTRODUCTION

The purpose of this study has been: (a) to investigate the processes involved in the mesoscale feedback process and effects of the feedback on the lower layers of the atmosphere; (b) to investigate the response of surface air to sea-surface properties; (c) to determine the "range of the coastal influence" and the effects of coastal fronts on the surface layers in the atmosphere; (d) to investigate the possibility of recognizing oceanic frontal effects with routine ship observations; and (e) to look into the accounting of feedback in numerical models.

To achieve the above mentioned objectives, descriptive physical models and theoretical considerations of heat and moisture transfer are used. These considerations are verified with specially designed field observations as well as with data from voluntary observing and reporting vessels.

The authors acknowledge the help of Mr. K. Rabe in the extraction and computer analysis of ship observations in the Labrador Current-Gulf Stream boundary region and of Mr. T. Harding in computing the sea-air temperature and water vapor pressure differences.

2. GENERALIZED FEEDBACK MODELS

A great number of different mathematical formulations can and have been established in the past to describe the energy cycle in the atmosphere and the ocean. The nature of each of the formulations depends on the types of numerical models used in the atmosphere and in the ocean. It is at times, however, useful to have a relatively complete, but simplified picture of the feedback system. An attempt is made to present such a schematic feedback cycle in Figure 1.

The essential factors and processes in large-scale considerations of the feedback cycle between the oceans and the atmosphere are:

(1) Rate of the uptake of moisture and latent and sensible heat due to surface winds and temperature/water vapor pressure differences between the sea surface and surface air.

(2) Transport and release of moisture and latent heat in the atmosphere. It should be emphasized that sensible heat effects are relatively small in the local uptake area. The circulation and release of latent heat in the atmosphere is one of the primary energy sources for the atmosphere.

(3) The horizontal gradients of heat and moisture in the atmosphere created by differential heating and cooling as a result of (1) and (2) above.

(4) The variation of storage and transport of heat by the ocean. This process is of special importance in causing weather anomalies in winter and early spring in higher latitudes.

(5) The effects on incoming and outgoing radiation by variations of cloud cover.

The feedback mechanism would change the energy circulation in different parts of the energy cycle either by magnification or reduction of its various effects. Most of these effects are handled in existing atmospheric PE (primitive equation) models with considerable simplification because of such factors as availability of computer time and core size, grid size, methods of solving of equations, etc. The energy input from the ocean to the atmosphere is introduced into the models at the surface and in some models this is only accomplished by introducing the sensible heat. Some boundary layer models offer greater detail than is possible in the hemispheric PE models. In these boundary layer models, however, the input is also effected in parametric form from the sea surface properties.

A mesoscale feedback model is presented in Figure 2. The most essential feature in this model is the direction (and speed) of the surface wind with relation to sea surface isotherms. This factor affects the resulting distribution of properties in the surface atmospheric layers as indicated in Figure 2. If the surface wind blows from the cold water side to the warm water side (the "providing cycle"), heat and moisture transport into the atmosphere is enhanced by bouyancy forces. If the wind blows from the warmer to colder side, the heat and moisture transport into the air is inhibited by increased stability (the "capping cycle") hindering the upward transport of heat and moisture. The radiative processes are less important in meso-scale feedback considerations than in large scale feedback models.

This paper is involved mainly with the type of model presented in Figure 2. This is essentially a generalized heat and moisture exchange model which emphasizes the response of the near surface air to the properties of the sea surface. Sea surface properties are relatively conservative as compared to the air, as the water source is unlimited and the heat capacity of the water is considerably higher than that of the air. Thus, essentially, this model deals with the response of the properties

of the surface air to the properties of the sea surface. This response can be expected to be most pronounced along the coasts where air masses from the continerts move over water surfaces which have greatly different properties than the initial properties of the air. Other areas of pronounced responses of surface air to the sea surface are the areas where strong thermal contrasts exist in the ocean, i.e., oceanic frontal regions. Some of these have been the subject of past studies (e.g., LaFond and LaFond, 1971).

3. THE RESPONSE OF SURFACE AIR PROPERTIES TO THE PROPERTIES OF THE SEA SURFACE

3.1 Theory

An air parcel moving over the sea surface, has its temperature and water vapor pressure changed mainly by the convective turbulent transfer of heat and moisture. If it is considered that the local change of sea-surface temperature is small, and assumed that the velocity of surface air particles is that of the surface wind speed, an equation for the change of sea-air temperature difference is obtained as follows:

$$\frac{d\Delta T}{dt} = \mathbf{W}\cdot\nabla T_w - \frac{dTa}{dt} \qquad (1)$$

where ΔT is $T_w - T_a$, i.e., the difference between sea surface and air temperatures and $\mathbf{W}\cdot\nabla T_w$ is the rate of change of sea surface temperature along the trajectory of the air. The same equation applied to water vapor pressure, except T is replaced with e (water vapor pressure). From observations (Mosby, 1933; and Bøyum, 1962) it has been found that the changes of air temperature can well be presented as:

$$\frac{dTa}{dt} = K(T_w - T_a) - C \quad . \qquad (2)$$

Substituting (2) into (1), rearranging and assuming $\mathbf{W}\cdot\nabla T_w$ to be constant, equation (1) can be transformed into integrable form:

$$\frac{d\Delta T}{dt} + K\Delta T = C + \mathbf{W}\cdot\nabla T_w \qquad (3)$$

which after integration gives:

$$\Delta T = \Delta T_o e^{-Kt} + \left(\frac{C}{K} + \frac{1}{K} V_r \frac{\partial T_w}{\partial r}\right)(1-e^{-Kt}) \qquad (4)$$

where r is the distance, ΔT_o is $T_w - T_e$ at the time t_o. The empirical constants of C and K must be determined from observational data.

Using K as 0.28 and C as 0.13, which is close to the values found by Bøyum (1962), assuming an initial sea-air temperature difference of 1.25°, and using various ΔT_w (i.e., the change of sea-surface temperature along the trajectory) it is found that the air temperature moving over the constant sea-surface temperature gradient reaches a constant value after about 5 hours travel (see Figure 3). Thus the response of the surface air properties to the properties of the sea surface is relatively fast. The final equilibrium sea-air temperature difference depends on the rate of change of sea-surface temperature ΔT_w along the trajectory of the surface wind.

It can generally be assumed that the transfer processes which move the moisture and heat upward from the surface are proportional to the rate of uptake of heat and moisture and that they do not cease when equilibrium conditions at the surface are reached. This upward transport rate must also change with the gradients of these properties with height in the atmosphere. There are relatively few measurements of this upward transfer rate; some indirect information about it can be drawn from time-series radiosonde observations. These observations with precision radiosondes indicate that the temperature profile, which mainly determines the stability, is the controlling factor of upward diffusion of heat and moisture. Furthermore, internal waves of temperature discontinuities seem to provide another important mechanism for upward transport of heat and moisture with "thermals."

It can be assumed that intensive feedback of energy from the sea to the atmosphere must affect the atmosphere itself locally and that these intensive exchange processes take place in certain meteorological conditions at oceanic fronts and in

coastal regions where large horizontal gradients in the underlying surface are present. Some theoretical studies of the feedback effects with relatively simplified assumptions have been carried out by Laevastu, Rabe and Hamilton (1972) which have demonstrated the local frontal effects on the atmosphere. Chapter 4 presents additional empirical evidence to verify the principal conclusions of the paper mentioned above.

3.2 Some Verifications of Surface Air Temperature and Water Vapor Pressure Computations

During the PATE (Pacific Thermal Experiment) expedition conducted by EPRF in November-December 1973 off the Central American coast, a 25 hour drifting station was occupied at the periphery of the Costa Rica Dome (mean position of the station was $10^0 00'N$; $88^0 10'W$). During this station both continuous recordings and half hourly measurements of various sea surface and surface air parameters were conducted. Among the measured parameters were sea-surface temperature, air temperature, "wet bulb" temperature and wind speed. Although the ship did not drift directly downwind, a possibility to estimate the change of sea-surface temperature under the trajectory of the wind was facilitated by continuous recording of sea-surface temperature and the drift of the ship. Other available surface oceanographic data were also used to check this sea-surface temperature gradient. Uncertainty in the estimate occurred at the beginning of the drift station and especially at the end of the drift station when a wind speed and direction change was experienced.

Using the measured data and the measured and/or estimated change of the sea-surface temperature along the trajectory of the wind, the surface air temperature and surface air water vapor pressure were computed (predicted) with formula 4. The computed data and the corresponding observed data are presented in Figures 4 and 5 as air-sea temperature difference ($T_a - T_w$) and air-sea water vapor pressure difference ($e_a - e_w$) respectively.

As Figure 4 indicates, Eq. (4) predicts the sea-air temperature difference reasonably well. Excluding the times where the rate of change of sea-surface temperature along the trajectory of the air could not be determined with great accuracy and when changes in wind speed and direction occurred (parts of curves marked with a and b), the standard error was about $\pm$ 0.2^{0}C. The relatively pronounced changes as well as several minor changes of ΔT in the observed values were also well reproduced.

The errors in surface air water vapor pressure differences (Figure 5) have the same causes as in the surface air temperature computation. Excluding the areas on the graph marked "a" and "b," the standard error of computing Δe with Eq. (4) was about $\pm$ 0.35 mb.

The above described verification test was carried out in an area with relatively sharp sea-surface temperature gradients and where the sea surface was colder than the air. Thus in more "normal" areas the prediction of T_a and e_a would be expected to be more accurate (see e.g., Bøyum, 1962). It could be pointed out that the T_a and e_a prediction requires good data on the surface wind both with respect to speed and direction as the term $V_r \frac{\partial Tw}{\partial r}$ in Eq. 4 has the greatest influence on the results.

4. SOME LOCAL EFFECTS OF SEA-AIR INTERACTIONS

4.1 Inversions in the Atmosphere

One of the peculiarities resulting from sea-air interaction in coastal and oceanic frontal regions is the temperature inversion in the atmosphere, especially off the west ccasts of continents and in the Mediterranean. Although all the conditions of the inversion are not necessarily due to local effects of sea-air interactions, the inversions, nevertheless, allow the evaluation of some aspects of the sea-air interaction processes. First, the layer between the temperature inversion (which occurs along the West Coast of the United States usually between 950 and 975 millibar levels) and the surface may be considered as the marine boundary layer. Figure 6 shows a temperature and humidity profile with an inversion layer off Point Arena, north of San Francisco. The relative humidity under the inversion is usually 100% and this is the place (and height) of formation of the California stratus. When the lower part of the marine layer is cooled, the stratus can reach the surface as fog. The inversion layer is a very good trap for the moisture as well as a heat flux barrier. When the inversion weakens or disappears, however, moisture can be transported upward in an "updraft" or "thermal." Such an updraft condition was indicated on 12 September and is presented in Figure 7.

Latest detailed radiosonde investigations by EPRF (using 3-hourly radiosondes, which were provided with a microswitch to give more details of the temperature and humidity structure) indicate that a pronounced stratification of humidity can exist in near-surface layers (surface to 850 mb level). Furthermore, rapid changes of this stratification occur and there are indications that the upward transport of moisture occurs intermittently in "updrafts" similar to "thermals" as well as with breaking internal waves at the temperature inversions. The detailed results of these studies will be published in the near future in another report.

4.2 Coastal Fronts and Range of Coastal Influence

The existence of thermal frcnts at the sea surface along coasts has been noticed for some time, although notes in literature about them are scarce. These fronts occur not only along upwelling coasts (see e.g., Bang, 1973) but along many continental and island coasts. In most cases they coincide quite closely with continental slopes or other sharp depth gradients (slopes). It has been generally assumed that the coastal oceanic fronts are causec by the interaction between dynamic and topographic features.

Several field investigations were conducted by EPRF to determine first the so-called "range of coastal influence" and secondly to ascertain the significance and the effect of coastal fronts on the atmosphere above in order to verify some theoretical and numerical studies on this subject reported earlier by Laevastu, Rabe, and Hamilton (1972). Some of the results of such recordings off Pcint Arena in September 1972 are presented in Figures 8 through 11. In Figure 8, it will be noticed that the properties of the sea surface and air come to typical oceanic equilibrium conditions seaward of the oceanic front. This front is well demarcated at about 26 n mi from the coast by sea-surface temperature as well as the temperature at 8 m depth. Towards the coast from this front, large differences between the air and sea surface properties exist which implies large heat and moisture fluxes. A rather noticeable feature in Figure 8 is the marked change of wind near the coastal front. Wind change at the oceanic fronts have been predicted by several theories (Laevastu, Rabe and Hamilton, 1972). A wind change at the coastal front has been observed in many sections (e.g., see Figure 10), though in some cases it is much less pronounced (see Figure 9). In Figure 9 will be seen a relatively complex thermal structure at the coastal front, the seaward end of which is about 38 n mi from

from the coast. This complex structure results from eddies and cutoffs from the different water types which is probably one of the main mechanisms of exchange of water between coastal and offshore areas. The sea and surface air properties reach a typical offshore equilibrium seaward from the front. Figure 10 shows the front only about 20 n mi from the coast with a marked change in winds near this front. The front obviously moves in tidal rhythm and is also influenced by wind regimes such as sea and land breezes.

The investigations of the oceanographic and meteorological coastal regime show that the coastal front can be considered as the outer edge of the so called "coastal influence." This coastal front and its outer edge also constitute, in most cases, the outer edge of the coastal upwelling regime. The edge of the upwelling is indicated in Figure 11 with the upward bending of the isotherms from 32 to 40 n mi from the coast.

The diurnal variability of the air properties is considerably larger between the front and coast than in offshore areas. It is especially large at the frontal region as indicated in Table 1. It would be an oversimplification to state that the coastal fronts are a consequence of coastal sea-air interactions alone as several other factors determine their positions (e.g., the continental slope). On the other hand, their importance in the feedback in the coastal zone is unquestionable. In this connection, it could be mentioned that the surface water between the front and coast is often warmer during summer and colder during winter. This seasonal relation does not, however, hold in the areas of coastal upwelling.

Table 1. Diurnal mean range of change of various meteorological and oceanographic parameters with distance from the coast on 12 to 14 September, 1972 off Point Arena. (T_w = sea-surface temperature; T_a = air temperature; T_{dd} = dew point depression).

Distance from the coast (km)	Range of observed change				
	T_w (°C)	T_a (°C)	T_{dd} (°C)	Wind speed, (knots)	Wind direction (deg)
0-15	1.7	2.3	1.5	11.0	53
15-45	2.5	3.5	2.0	15.6	137
45-60	0.7	1.4	1.3	10.0	50

These coastal zone investigations, furthermore, substantiate the theoretical computations on the speed of the change of the surface air properties in response to sea surface properties. The verification indicates that the response of the surface air to the properties of the sea surface might even be somewhat faster than the theoretical computations of the authors (Laevastu, Rabe and Hamilton, 1972). This can be noticed in Figures 4 and 5 and in Figures 8 through 10, where the trends and rate of change of sea-surface temperature (T_w) and air temperature (T_a) are quite closely related at the coastal frontal area.

4.3 Oceanic Frontal Effects as Revealed by Synoptic Data from Merchant Ships

Synoptic ship reports from the Labrador Current-Gulf Stream boundary region off Newfcundland were analyzed in 10-day composite analyses for May, June, October and November 1968. Due to the scarcity of data, the relatively coarse (381 km) standard numerical hemispheric meteorological grid was used. This coarse grid would not allow accurate presentation of the very sharp thermal front which exists in this area.

Despite the shortcomings in the accuracy of the data, low data density and large grid size, the results indicate indirectly a relatively rapid response of surface air to the properties of sea surface. This relatively rapid response can be recognized by comparing the sea-surface temperature, air temperature and dew point temperature charts for 11 to 20 May 1968 in Figures 12 through 14. The greatest difference between the sea surface and air temperatures is found in the general area of the oceanic front (Figure 15). Figure 16 shows that the observed winds are also strongest at the oceanic frontal regions -- as earlier observed by Cormier and Kindle (1971) and as predicted from the theoretical considerations by Laevastu, Rabe and Hamilton (1972). The ten-day composite geostrophic winds for the period 11 to 20 May 1968 in the Labrador Current-Gulf Stream boundary area are shown in Figure 17. A comparison of Figures 16 and 17 indicates that the observed surface winds at the oceanic frontal region deviate considerably from the computed geostrophic winds, a fact briefly pointed out by Roll (1965).

Figure 18 shows the computed latent heat (Q_e) exchange in the area under consideration during the period 11 to 20 May 1968 (g cal/cm^2/24h). The sharper gradient of Q_e coincides with the oceanic front, as expected.

Figure 19 shows the analysis of observed surface wind speed from 1 to 10 June 1968 in the area under consideration. Again the stronger winds occur at the oceanic frontal region, similar to the conditions twenty days earlier (shown ir Figure 16).

Figure 20 gives the composite sea-surface temperature analysis for the ten-day period 11 to 20 November 1968 in the Labrador Current-Gulf Stream boundary area. Figure 21 shows the sea surface and air temperature difference for the same period and area as the previous figure. Again, the difference of temperatures of air and sea is largest at the oceanic front, thus the same condition as observed in May (Figure 15).

The observed wind speed at the frontal region (Figure 22) is again stronger than the computed geostrophic wind in Figure 23. The observed strongest wind band also follows the general position of the front.

In summarizing the essentials of the above studies, it is apparent that (a) the observed winds are most often stronger near the oceanic fronts than on either side of it and (b) that near the oceanic fronts the difference between computed geostrophic wind and observed wind are larger than in other areas. This seems to verify the effects of the frontal zone on the atmosphere above, as computed theoretically by Laevastu, Rabe and Hamilton (1972).

5. NOTES ON ACCOUNTING OF SEA-AIR INTERACTIONS IN BAROTROPIC AND MEDIUM RANGE ANALOG MODELS

The barotropic models of the atmosphere in use for numerical prediction have been, by necessity, greatly simplified. The barotropic condition does not allow for vertical wind shear and excludes horizontal temperature advection and the baroclinic processes associated with it. In spite of the simplified assumptions, the barotropic 500 millibar predictions have been surprisingly successful. Their quality is about the same by filtered and unfiltered models (Reiser, 1973; and Edelmann, 1973). Some barotropic model tests with "artificial" effects such as the inclusion of feedback of energy from the ocean to the atmosphere have given only slightly better results in the past. On the other hand, there are also considerable shortcomings in primitive equation (PE) models at present. The approximation of some physical processes and large grid sizes in numerical calculations affect the results. For example, the sensible heat addition from the surface has no effect on the vertical advection in the hydrodynamic equation because of the finite difference methods used (Danard, 1971).

Relatively incomplete experiments with the addition of feedback effects have been made with large scale numerical atmospheric models. However, the feedback processes and effects are essentially mesoscale phenomena. On the other hand, the testing of the inclusion of feedback processes and effects into the PE model could best be effected via a separate boundary layer model. The latter must, by necessity, be relatively complex, however, and the experimentation and testing of feedback formulations in such boundary layer models is an extensive task. Furthermore, such models require very accurate and detailed knowledge of the initial state which is not possible with the presently available synoptic data density and with large changes of the temperature and humidity profiles near the surface.

At EPRF, it is planned to test the feedback effects in a fine scale "window" model. The grid size in such tests will be small because of the relatively small-scale processes in the coastal zone and in frontal regions. The feedback can be in terms of quantitative energy flow, as determined by the relations between the surface wind and the sea-surface temperature isotherms.

A further challenging possibility for testing and application of the feedback effects is in the improvement of the medium range analog forecasts. In these models, the feedback input must be in a simplified empirical parametric form and mainly in terms of the resulting effect of the latent heat feedback on the behavior of the atmosphere downstream. This requires the identification of the areas of latent heat exchange anomalies. Work in these subjects is in progress at EPRF.

6. SUMMARY

(1) In a large-scale ocean-atmosphere feedback system the important factors in influencing and determining the energy gradients in the atmosphere are: (a) the rate of uptake of moisture (latent heat) from the sea, (b) heat storage and transport by ocean currents, (c) moisture transport by the air, (d) release of latent heat, (e) the direction of the surface wind with relation to sea surface isotherms and the winc speed and (f) the modifying effects of clouds on radiation prccesses. In small scale models (dealing mainly with local exchange processes) the important factors are: (a) the direction of the surface wind with relation to sea surface isotherms and the gradients of the latter, along the trajectory of the surface air, (b) the initial difference in the properties of sea surface and surface air (especially important in coastal areas), and (c) the local effects of the heat and moisture uptake (e.g., stability changes near the surface).

(2) The properties of the surface air (T_a and e_a) can be computed with the Åmot - Mosby formula. The response time of the surface air is rapid (ca., 5 hours). The standard error in T_a computation is about 0.2°C and in e_a computation about 0.35 mb. These formulas should be used in numerical atmospheric models.

(3) Among the noticeable local sea-air interactior phenomena is the formation of coastal stratus and fog which forms off the California coast under the inversion layer.

(4) The coastal oceanic front (usually 10 to 50 n mi from the shore) forms the outer limit of the "range of coastal influence."

(5) The difference between the sea surface and surface air properties is large between the coast and coastal front, implying also large heat and moisture exchange in this area. The diurnal change of surface air properties is also large in the same area.

(6) There is often a marked wind change in the vicinity of the coastal front due, not only to the feedback effects at the front, but also to the front being a boundary of the sea-land wind regime.

(7) Pronounced feedback effects of oceanic fronts on the surface winds appear also in ten-day composite analyses of ship reports. The winds at the major oceanic frontal zones are stronger than on either side of it. These stronger winds do not appear in computed geostrophic winds in oceanic frontal zones.

(8) The feedback effects in numerical atmospheric models can be accounted for in three principal ways:

(a) By the inclusion of local heating (and moisture addition) in parametric form -- the main controlling parameter being wind direction (and speed) with relation to sea surface isotherms.

(b) In mesoscale models (including boundary layer models), the individual heat exchange components must be quantitatively included and their immediate and short-range effects computed. This requires, however, the assessment of initial state (analysis) in great detail, which is not possible with the present density and quality of synoptic observations and because of relatively large spacial and temporal changes.

(c) In medium range analog models, the feedback (mainly latent heat source) must be included empirically via its known quantitative effects. This task is of great practical utility.

REFERENCES

Bang, N.D., 1973: Characteristics of an intense ocean frontal system in the upwell regime west of Capetown. Tellus 25, 25 (3):256-265.

Bøyum, G., 1962, "A Study of Evaporation and Heat Exchange Between the Sea Surface and the Atmosphere." Geofys. Publ., (Geophys, Norv.) 22, 7:15 pp.

Cormier, R.V. and E.C. Kindle, 1971: Diagnoses and prediction of marine boundary layer mesoscale wind phenomena. Proc. Techn. Conf. Autom. Weather Support, Air Wea. Serv. Techn. Rpt. 242:98-111.

Danard, M.B., 1971: A numerical study of the effects of longwave radiation and surface friction on cyclone development. Monthly Weather Rev. 99, (11): 831-839.

Edelmann, W., 1973: Barotrope Modelle mit Larmfilterung Promet, Meteorologische Fortbildung, Frankfurt, Heft 1: 11-15.

Laevastu, T., K. Rabe, and G.D. Hamilton, 1972: The effects of oceanic fronts on properties of the atmospheric boundary layer. EPRF Tech. Paper 2-72: 46 pp.

Laevastu, T., 1973: Coastal sea-air interactions and the extent of coastal influence. Progress report 2. EPRF Tech. Note 8-73:32 pp.

LaFond, E.C. and K.G. LaFond, 1971: Thermal structure through the California front. Naval Undersea Center, San Diego, TP 224:133 pp.

Mosby, H., 1933, "The Sea Surface and the Air." Scient. Rep. Norw. Antarct. Exp. 1927-1928, 10:140 pp.

Reiser, H., 1973: Barotrope Vorhersagemodelle ohne Larmfilterung Promet, Meteorologische Fortbildung, Frankfurt, Heft 1:6-10.

Roll, H.U., 1965: Physics of the Marine Atmosphere, Academic Press, London 426 pp.

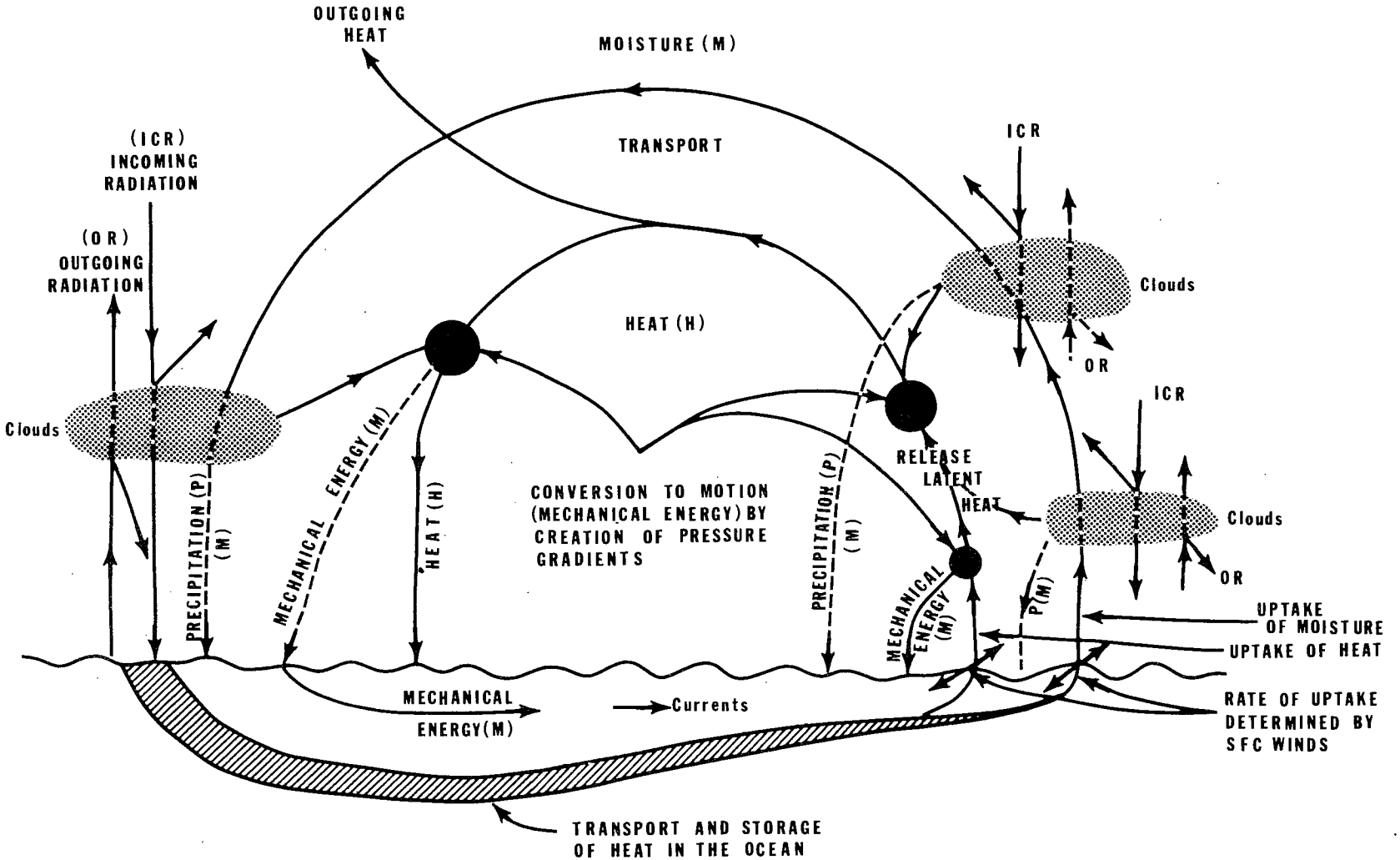

Figure 1. Schematic presentation of large scale feedback cycle.

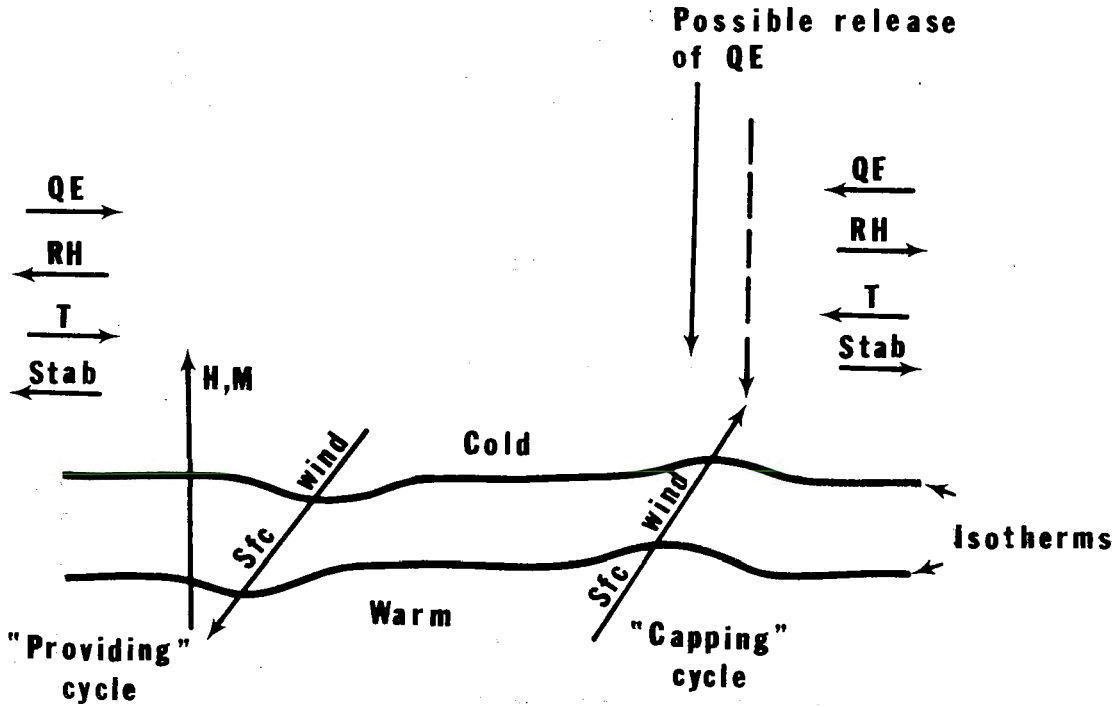

Symbols: ⟶increase; ⟵ decrease; H-heat; Sfc-surface; M-moisture; T-temperature QE-Latent heat; RH-relative humidity; Stab-stability.

Figure 2. Generalized mesocale feedback model with indication of the effects on the changes of properties of boundary layer.

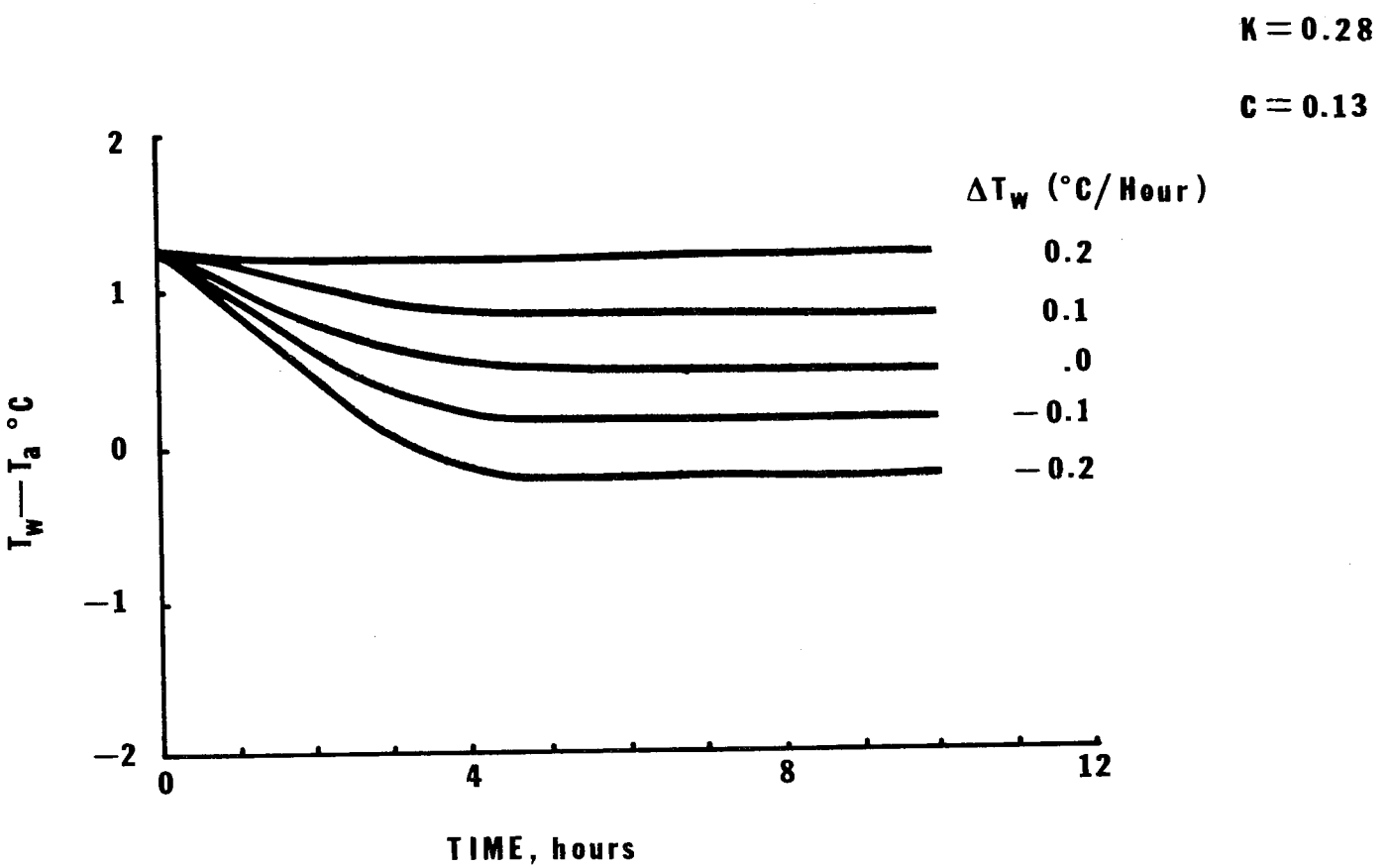

Figure 3. Change of sea-air temperature difference (ΔT) with time and with different rate of change of sea surface temperature under the trajectory (ΔT_w). C=0.13; K=0.28, initial $\Delta T = 1.25^{o}C$ (Formula 4).

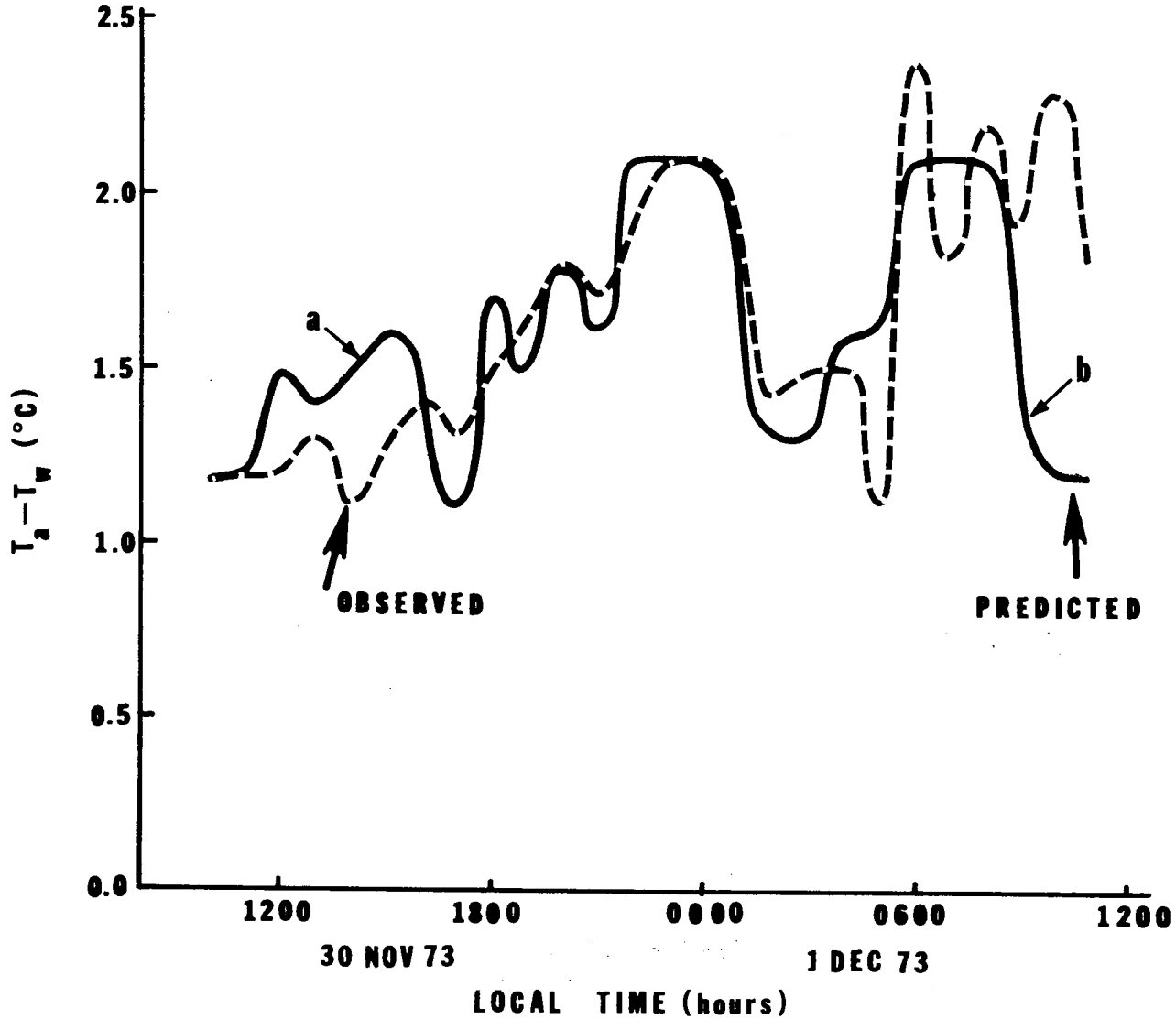

Figure 4. Observed and computed air-sea temperature difference during a drifting station at the periphery of Costa Rica Dome (mean position 10°00'N; 88°10'W) during 30 November and 1 December 1973. C=0.10, K=0.35.

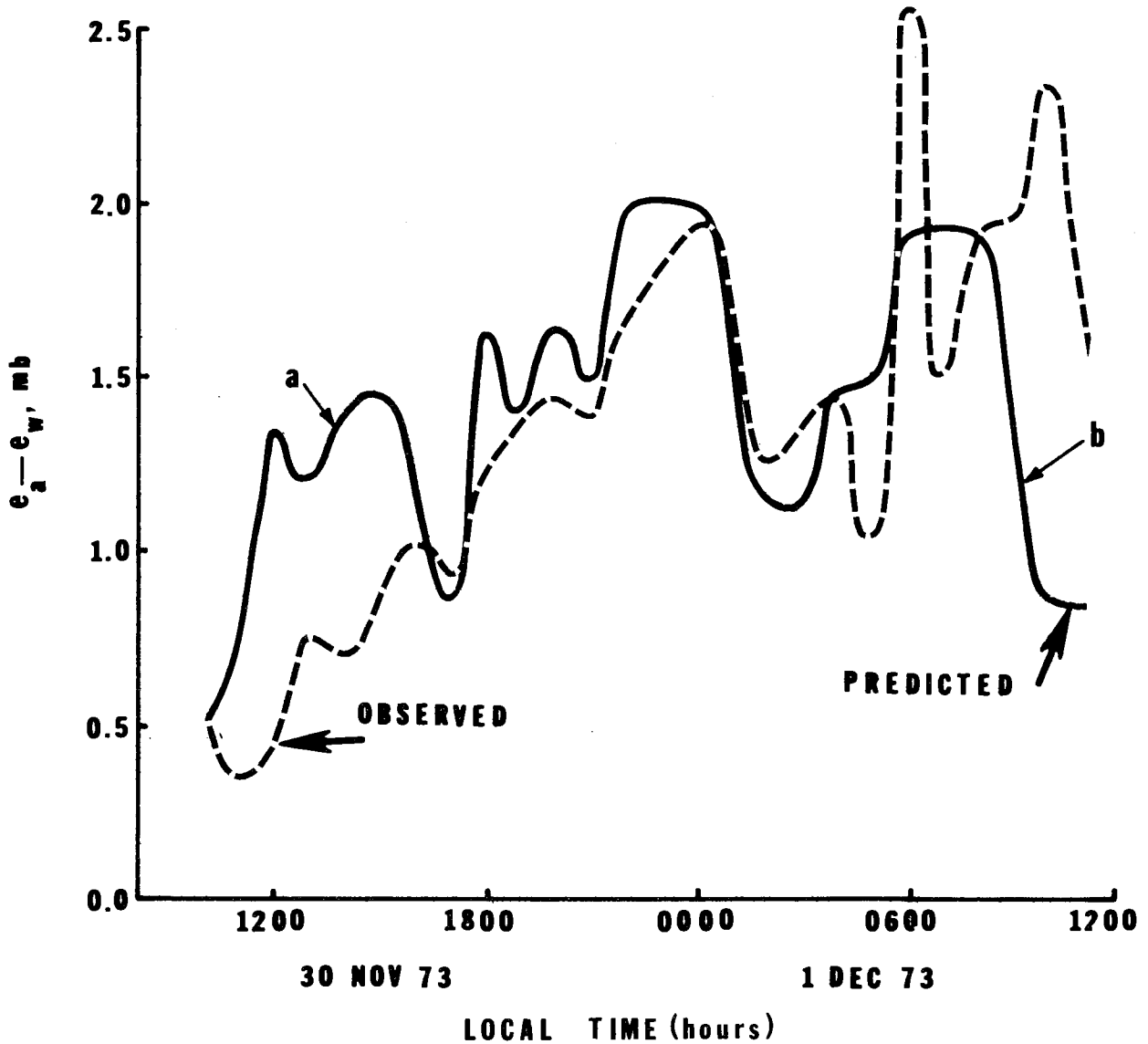

Figure 5. Observed and computed air-sea water vapor pressure difference during a drifting station at the periphery of Costa Rica Dome (mean position 10°00'N; 88°10'W) during 30 November and 1 December 1973. C=0.40; K=0.50.

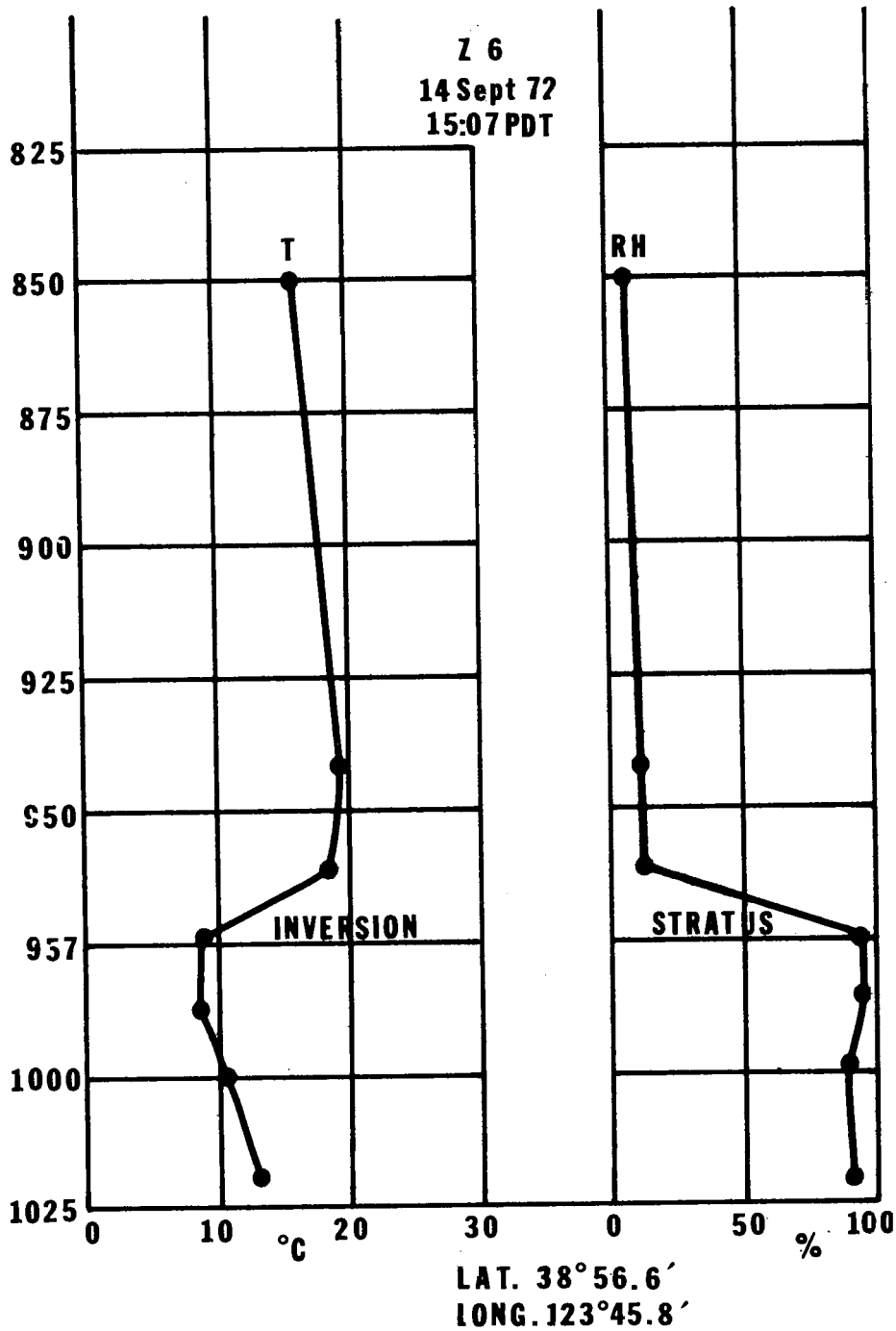

Figure 6. Temperature (T) and relative humidity (RH) profiles off Point Arena, 1507 on 14 September 1972.

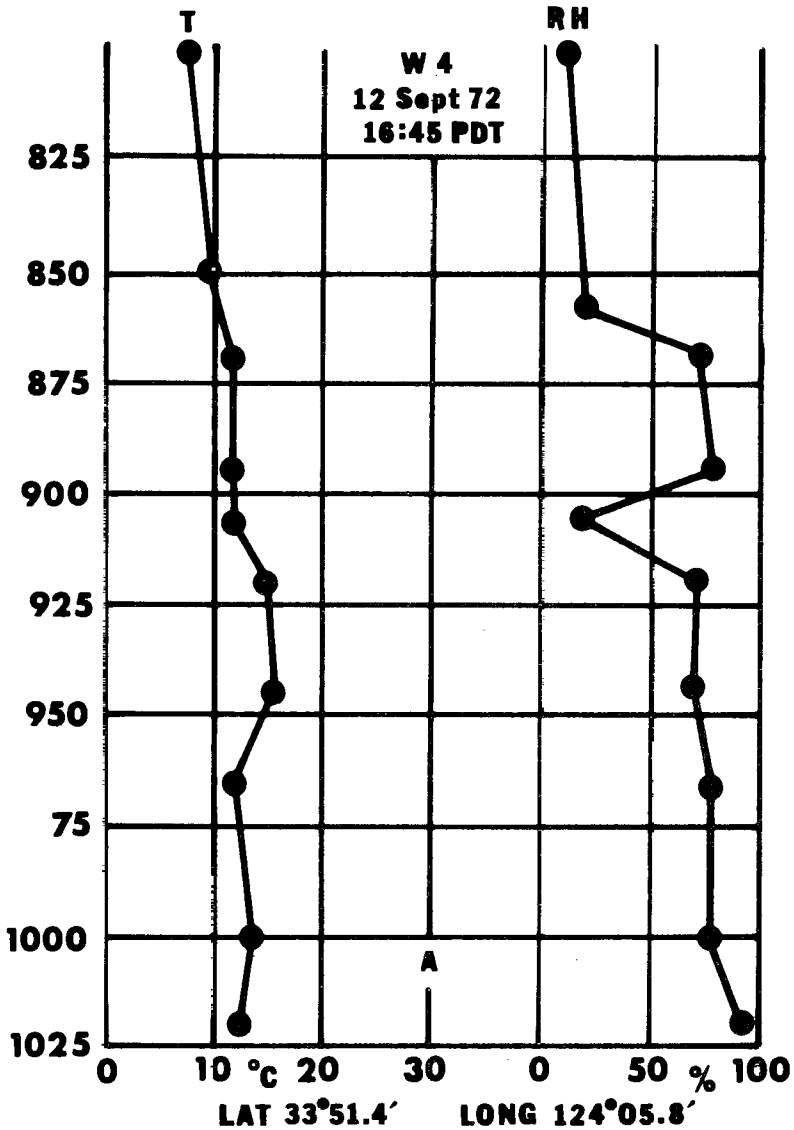

Figure 7. Temperature (T) and relative humidity (RH) profiles off Point Arena, 1645 PDT on 12 September 1972.

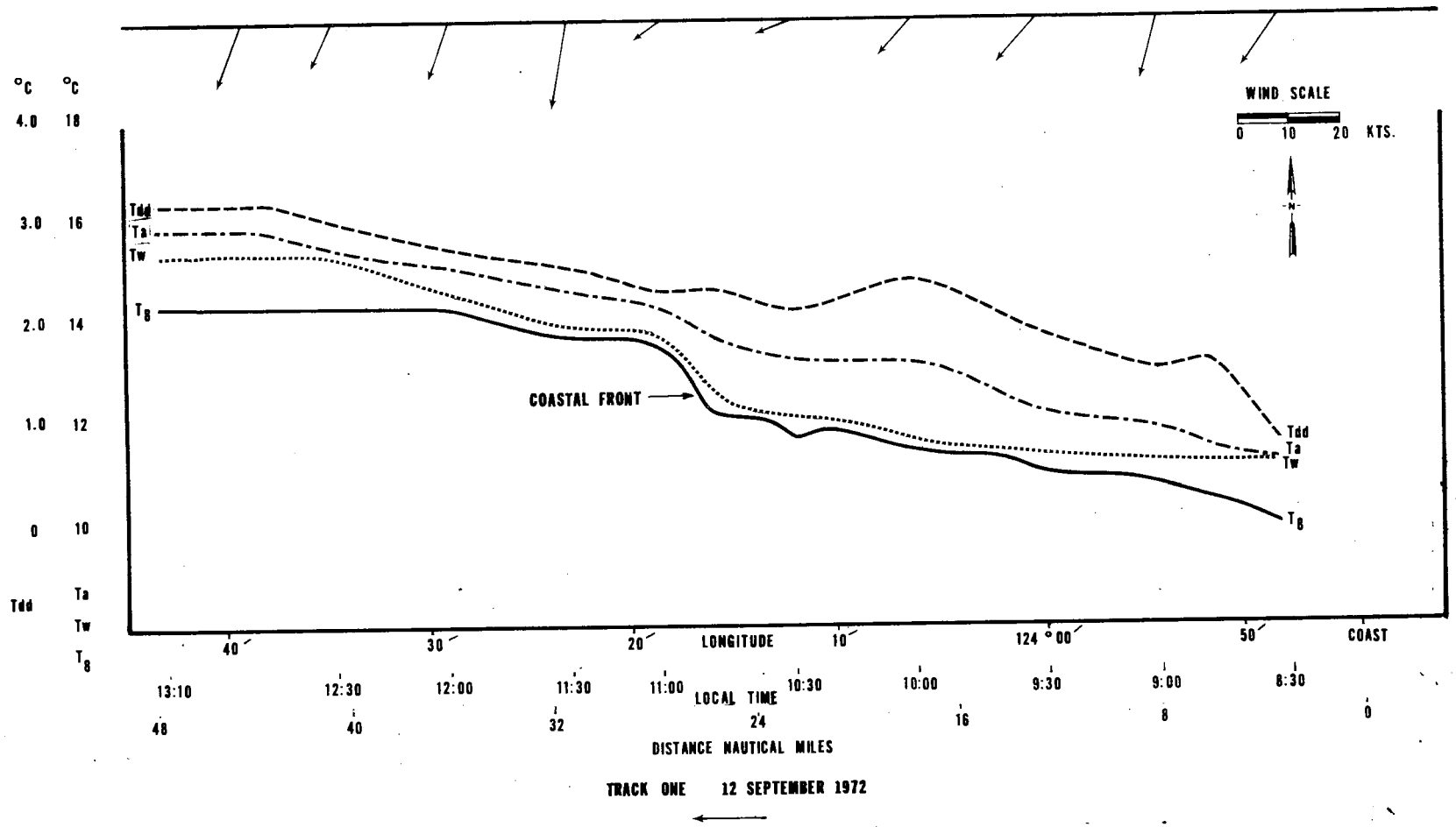

Figure 8. Sea surface temperature (T_w), temperature at 8 feet (2.4m) depth (T_8), air temperature (T_a), dew point depression (I_{dd}) and wind direction and speed off Point Arena, from coast to 48 nautical miles offshore, 0830 to 1310 PDT on 12 September 1972.

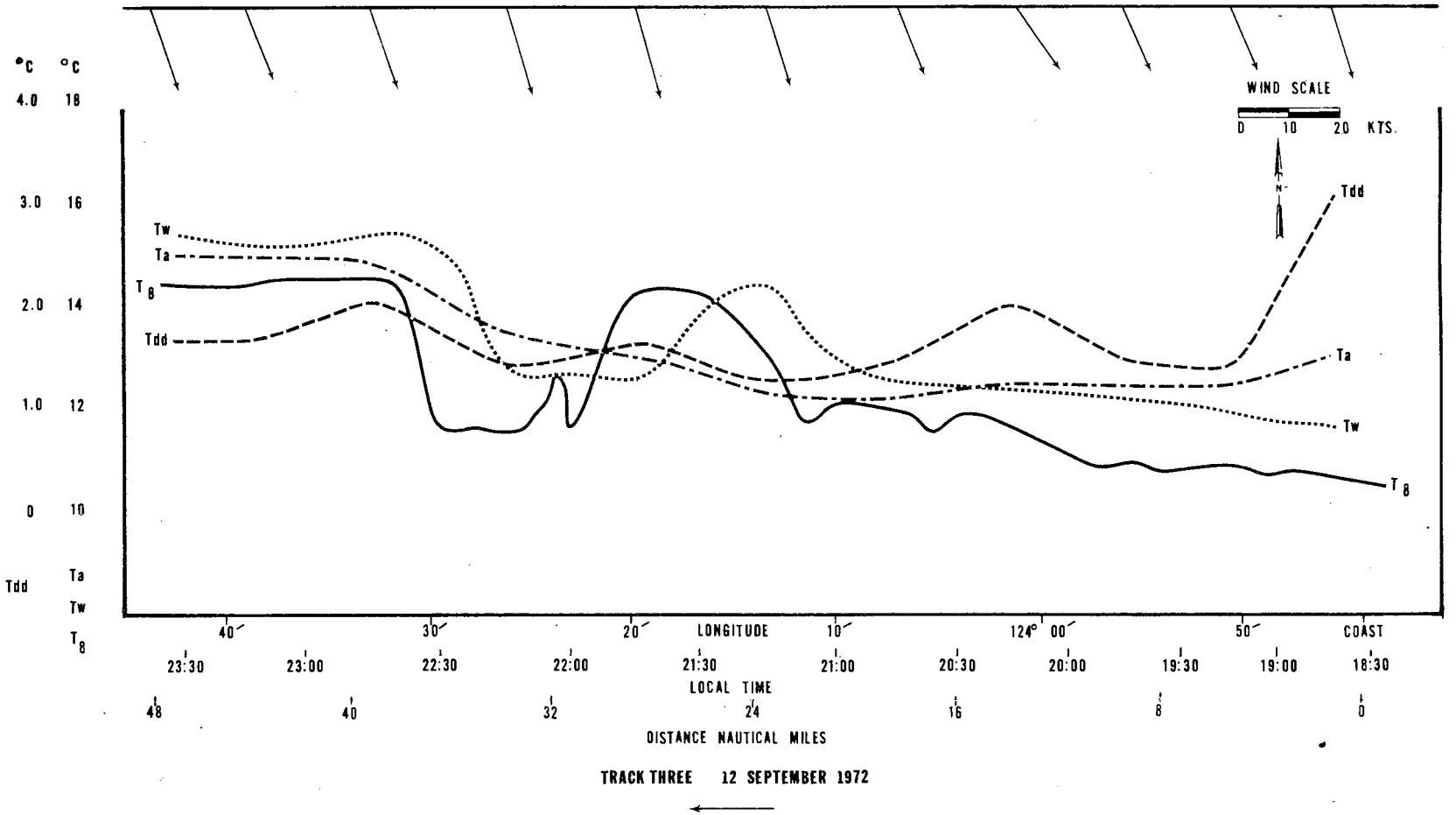

Figure 9. Sea surface temperature (T_w), temperature at 8 feet (2.4m) depth (T_8), air temperature (T_a), dew point depression (T_{dd}) and wind direction and speed off Point Arena, from coast to 48 nautical miles offshore, 1830 to 2330 PDT on 12 September 1972.

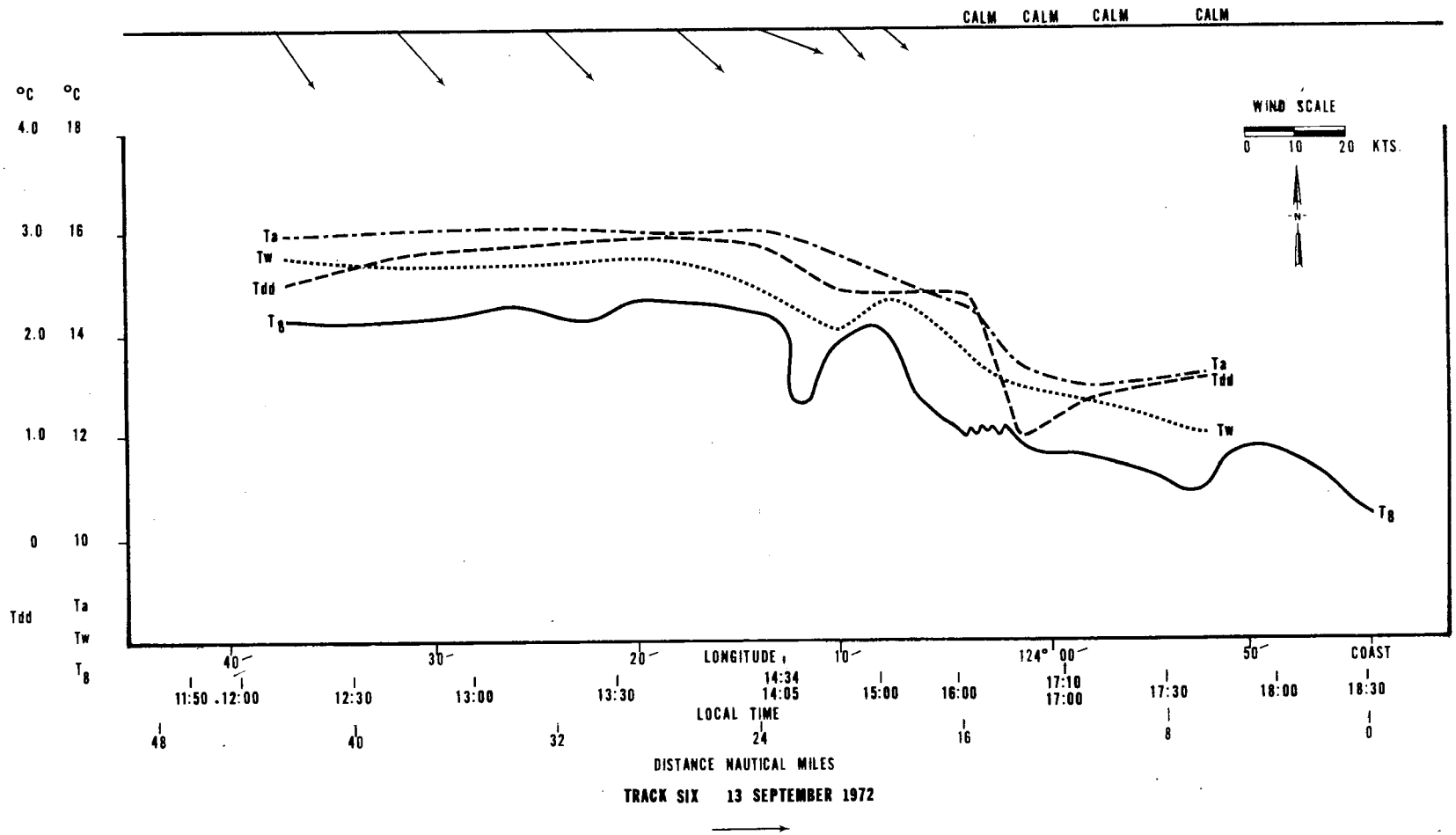

Figure 10. Sea surface temperature (T_W), temperature at 8 feet (2.4m) depth (T_8), air temperature (T_a), dew point depression (T_{dd}) and wind direction and speed off Point Arena, from coast to 48 nautical miles offshore, 1150 to 1830 PDT on 13 September 1972.

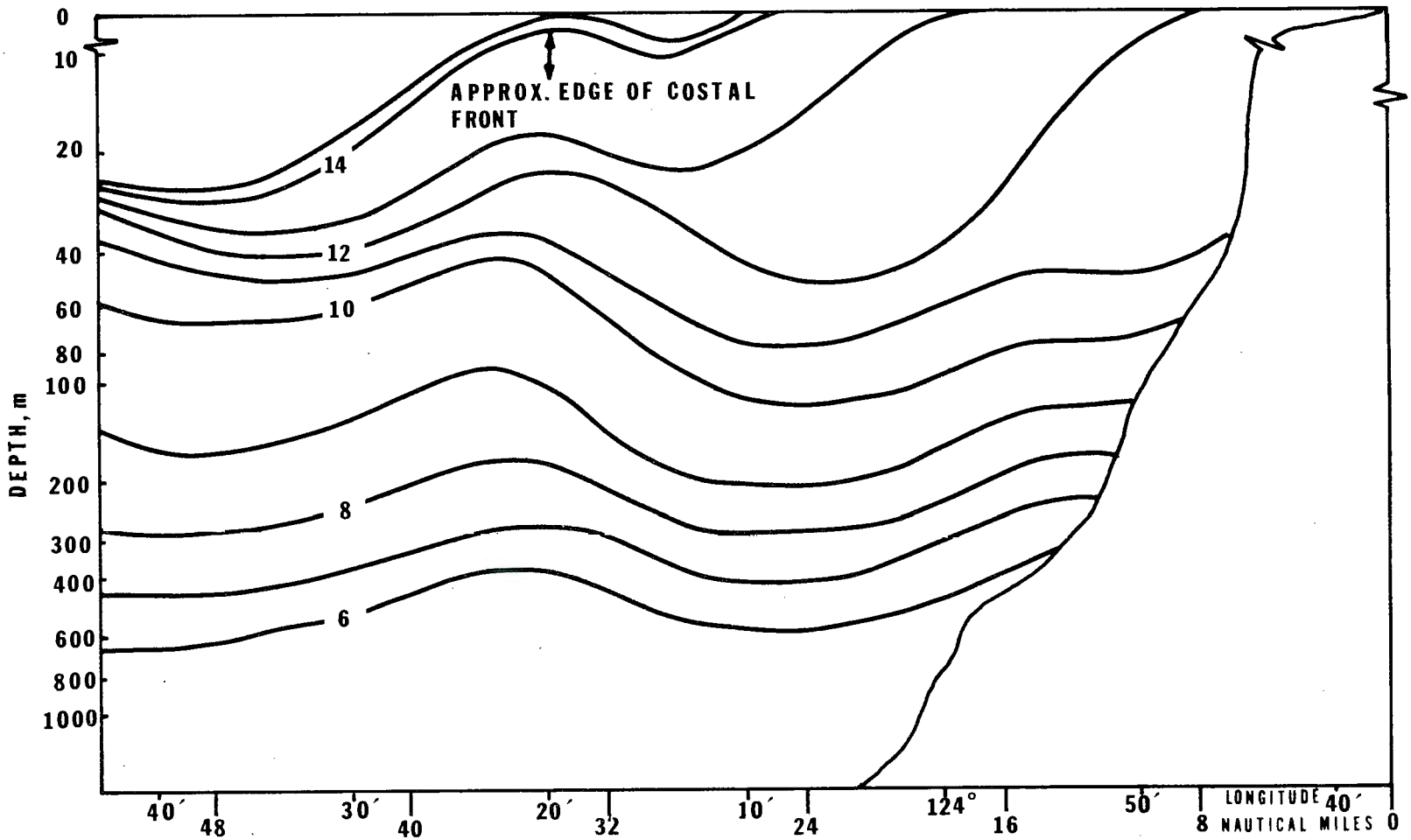

Figure 11. Depth of isotherms along a section from the coast to 50 nautical miles offshore off Point Arena, 0950 to 1507 PDT on 14 September 1972.

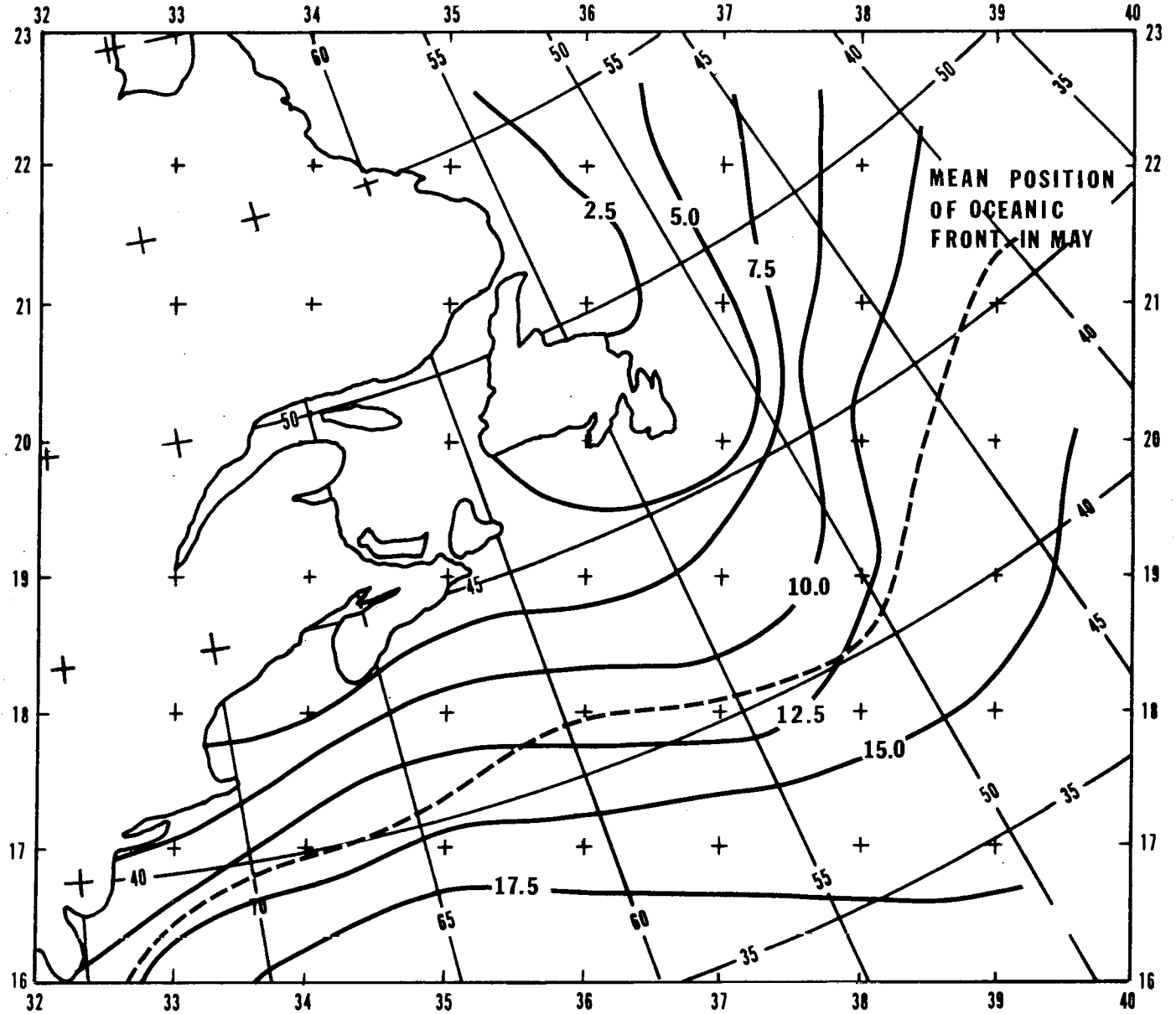

Figure 12. 10-day composite sea surface temperature (^{o}C) analysis from ship reports in Labrador Current-Gulf Stream boundary area, 11 to 20 May 1968.

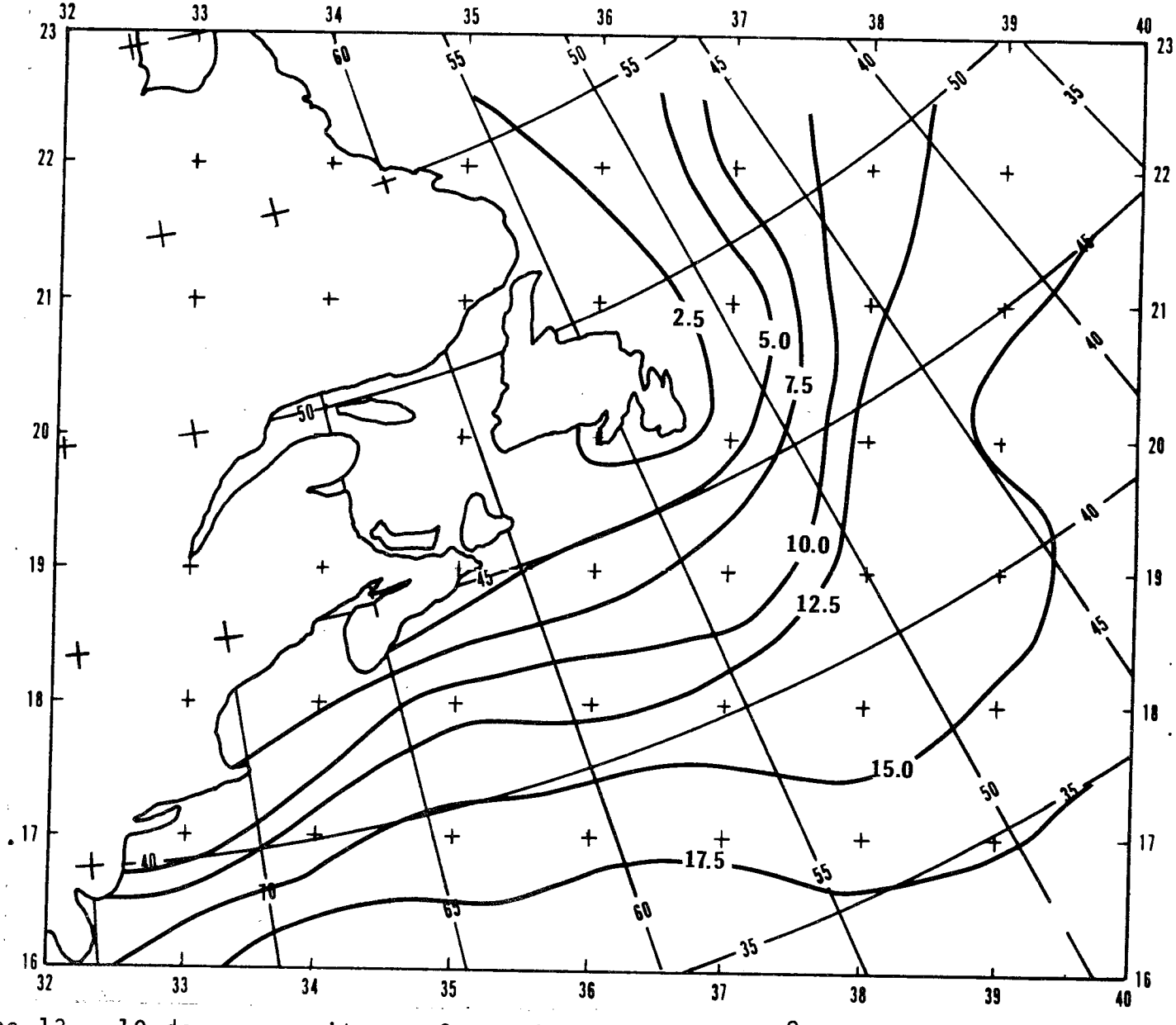

Figure 13. 10-day composite surface air temperature (^{o}C) analysis from ship reports in Labrador Current-Gulf Stream boundary area, 11 to 20 May 1968.

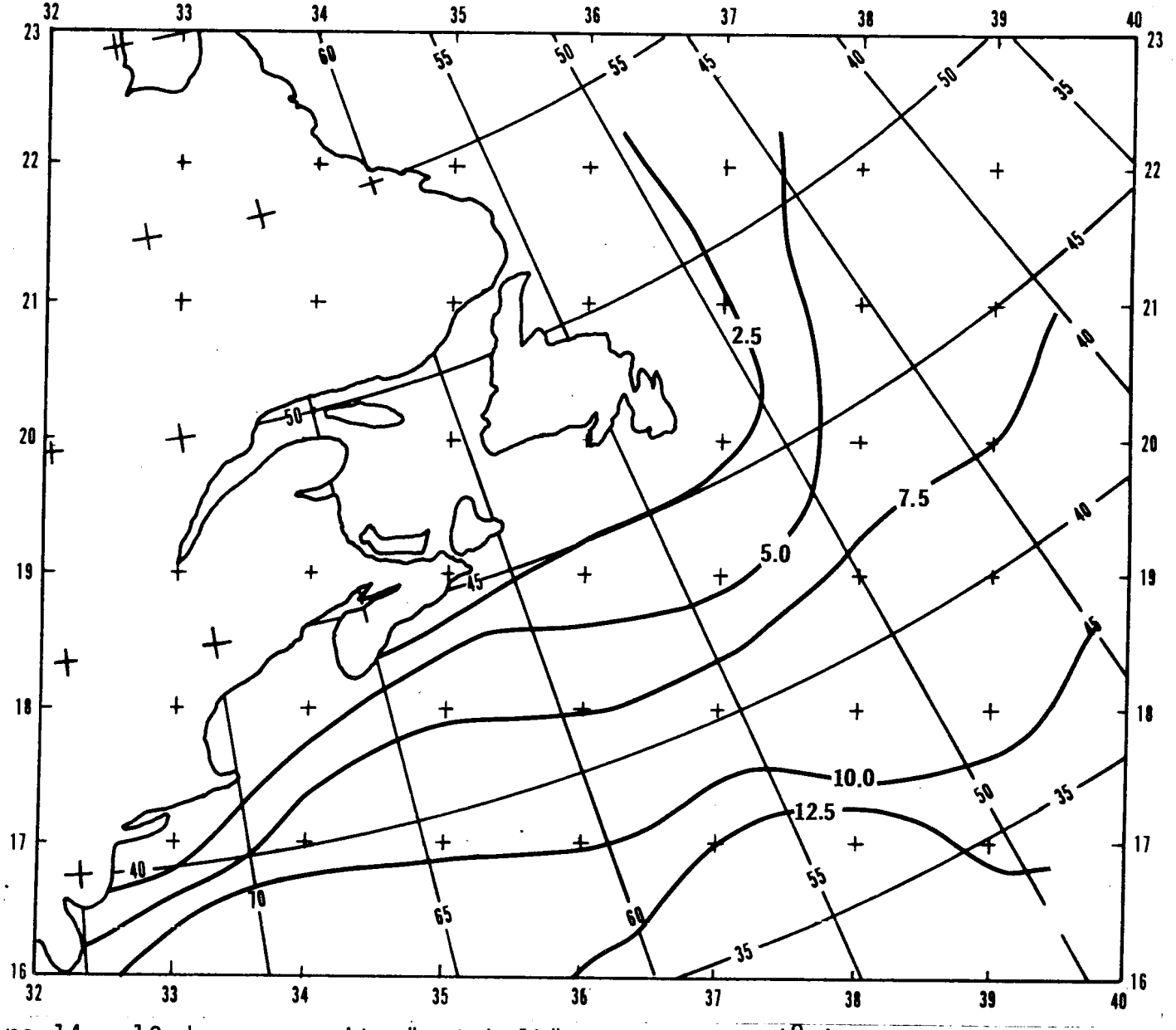

Figure 14. 10-day composite "wet bulb" temperature (^{o}C) analysis from ship reports in Labrador Current-Gulf Stream boundary area, 11 to 20 may 1968.

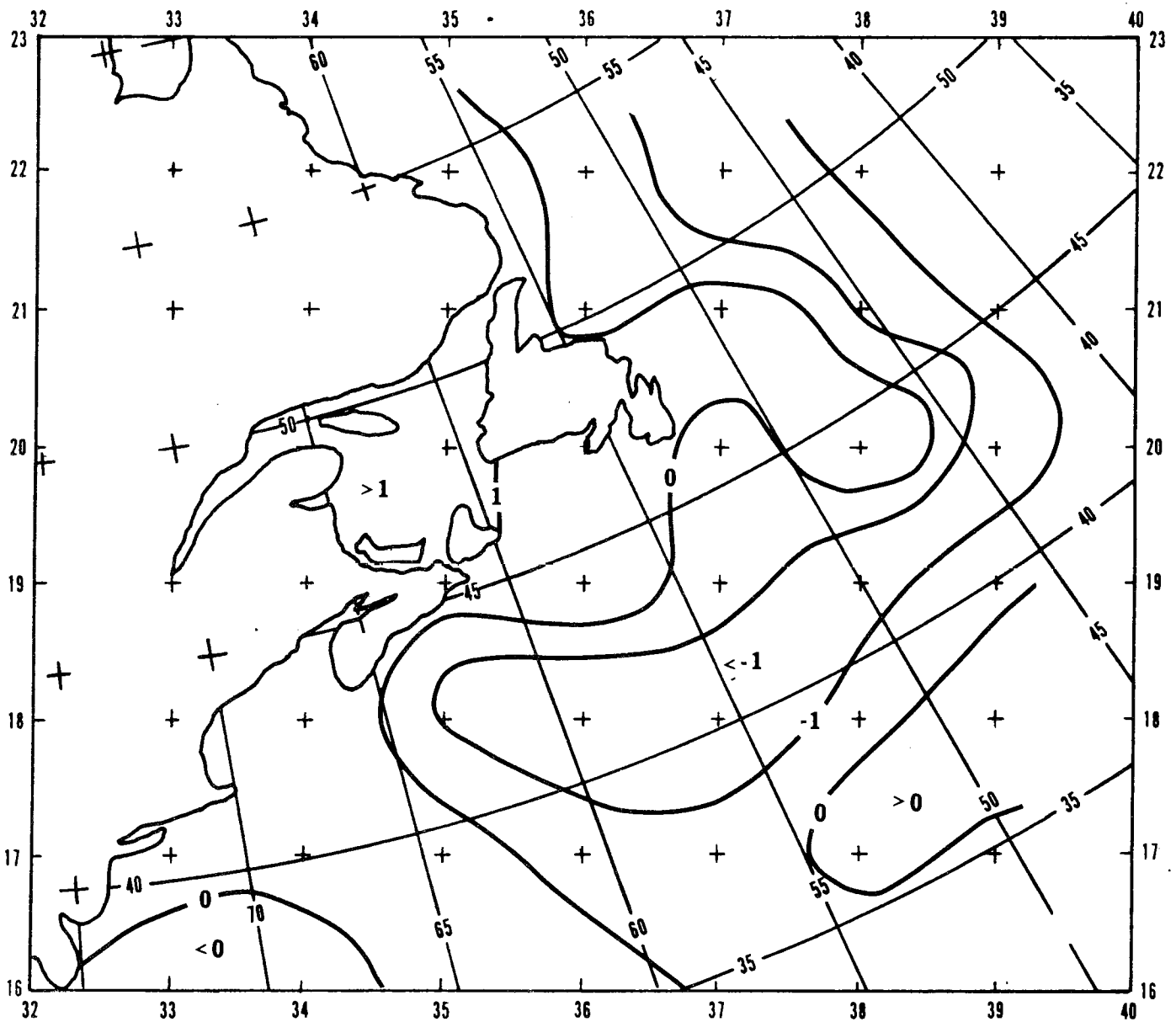

Figure 15. 10-day composite sea surface and surface air temperature difference (^{o}C) analysis from 11 to 20 May 1968.

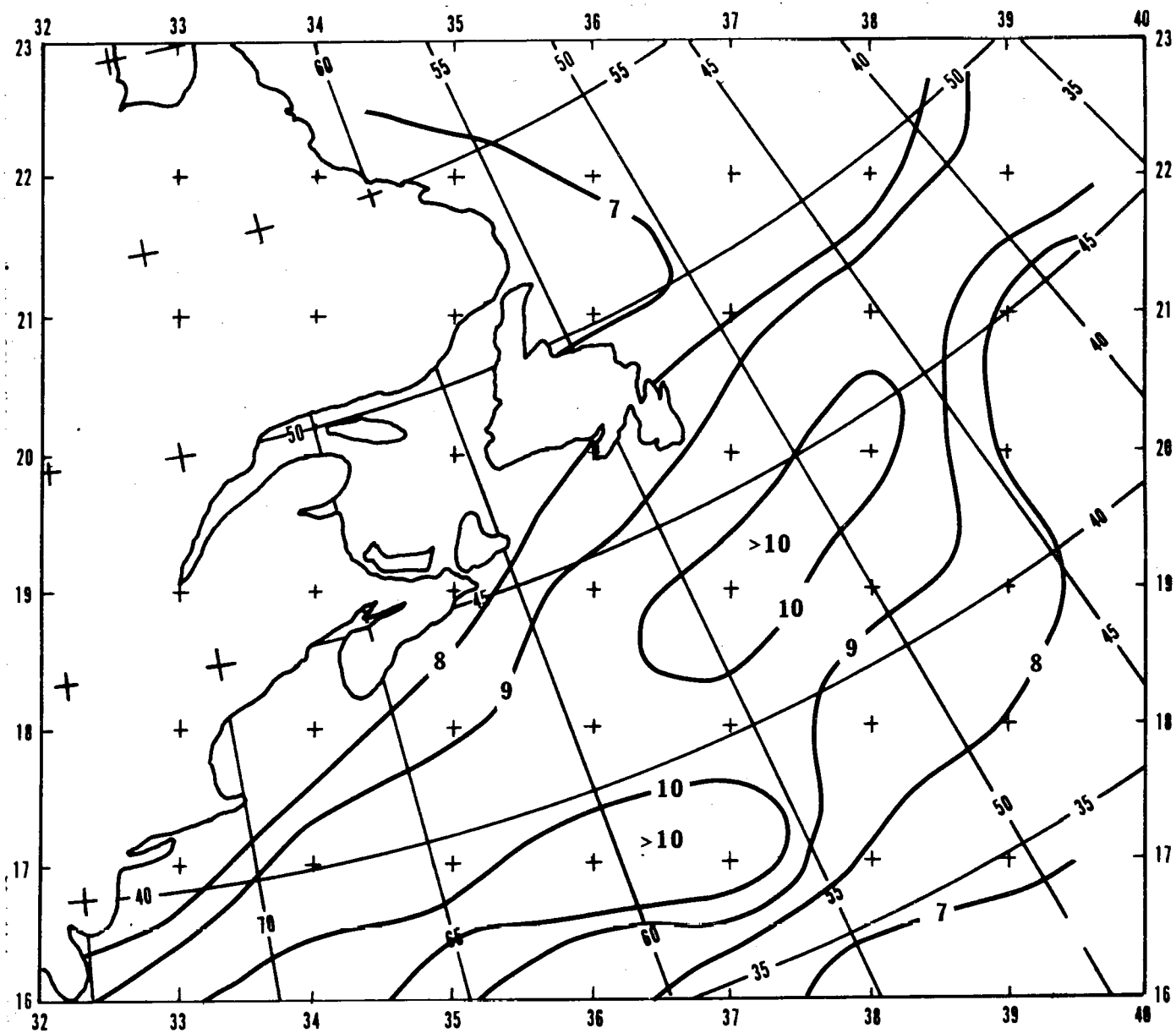

Figure 16. 10-day composite surface wind speed (m/sec) analysis from ship reports in Labrador Current-Gulf Stream boundary area, 11 to 20 May 1968.

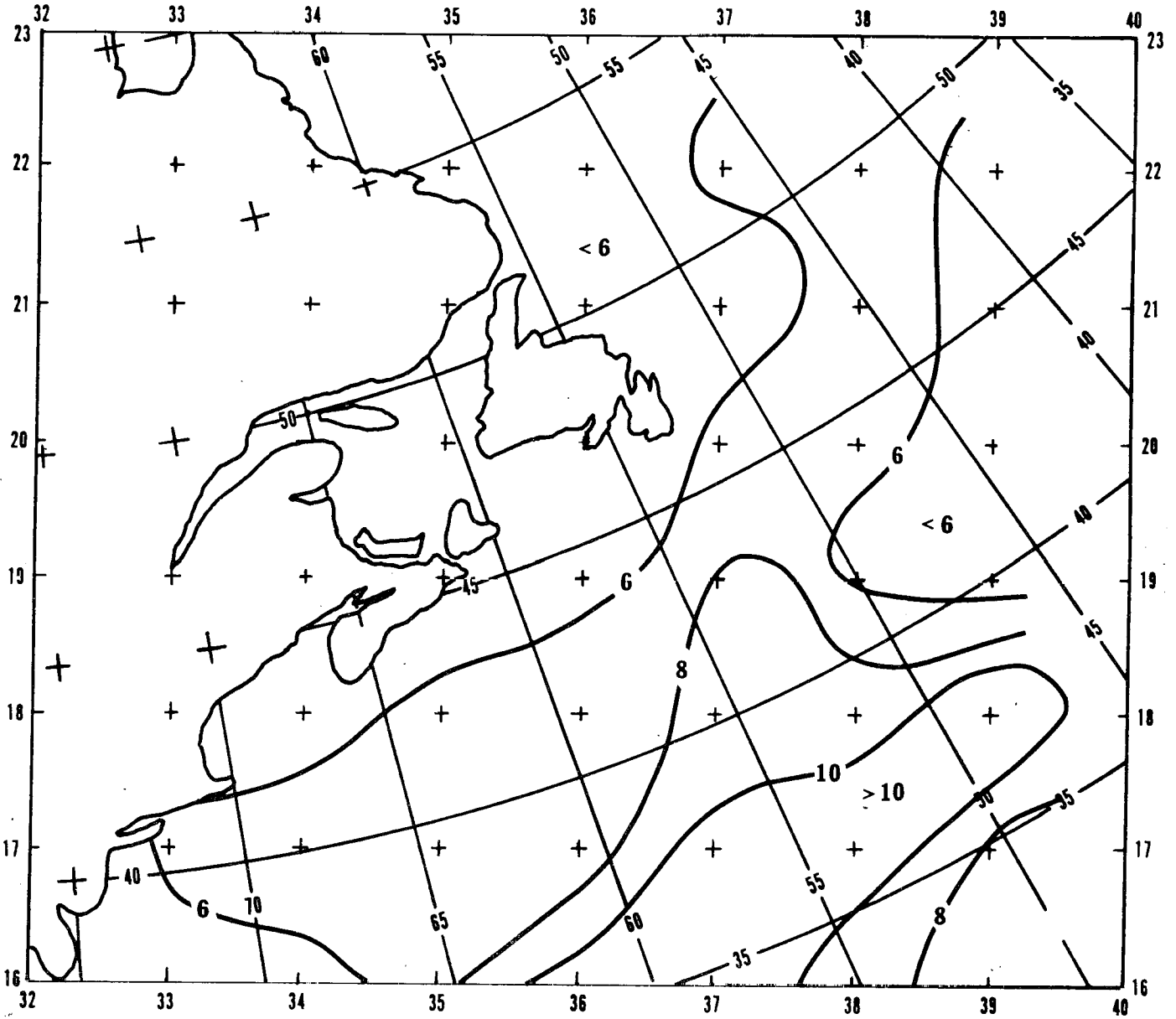

Figure 17. 10-day composite geostrophic wind speed (m/sec) analysis in Labrador Current-Gulf Stream boundary area, 11 to 20 May 1968.

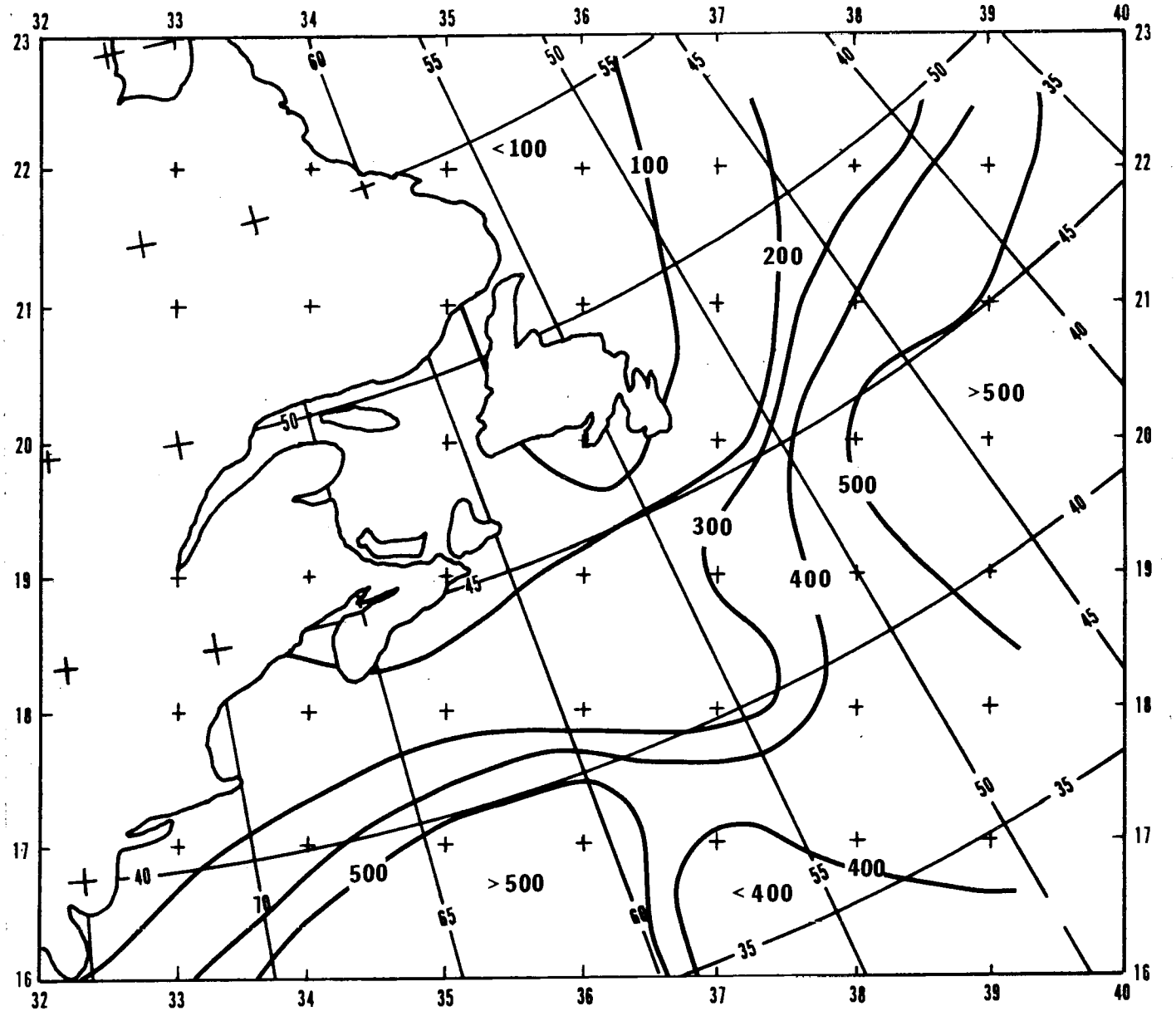

Figure 18. 10-day composite latent heat exchange in Labrador Current-Gulf Stream boundary area 11 to 20 May 1968.

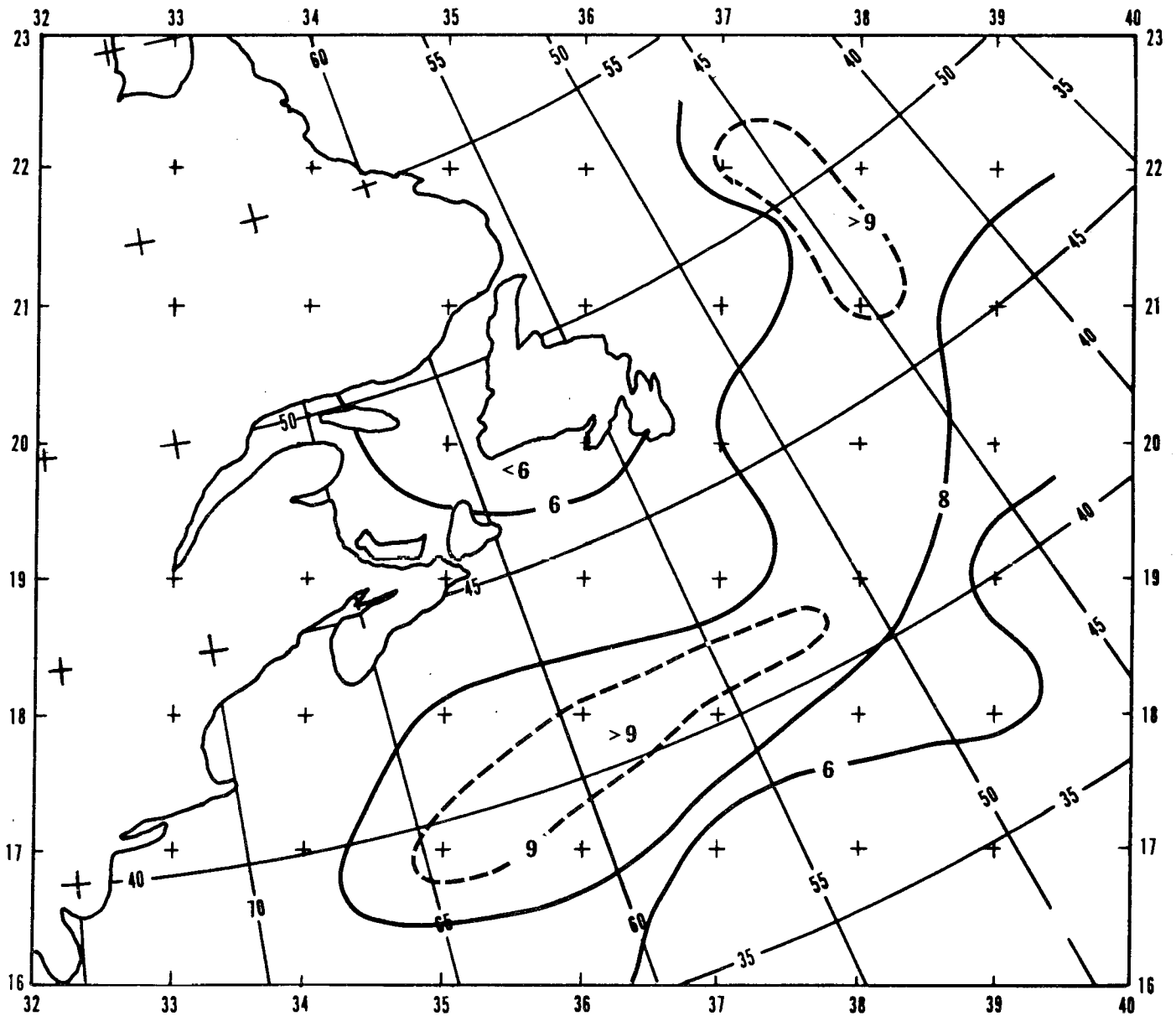

Figure 19. 10-day composite surface wind speed (m/sec) analysis from ship reports in Labrador Current-Gulf Stream boundary area 1 to 10 June 1968.

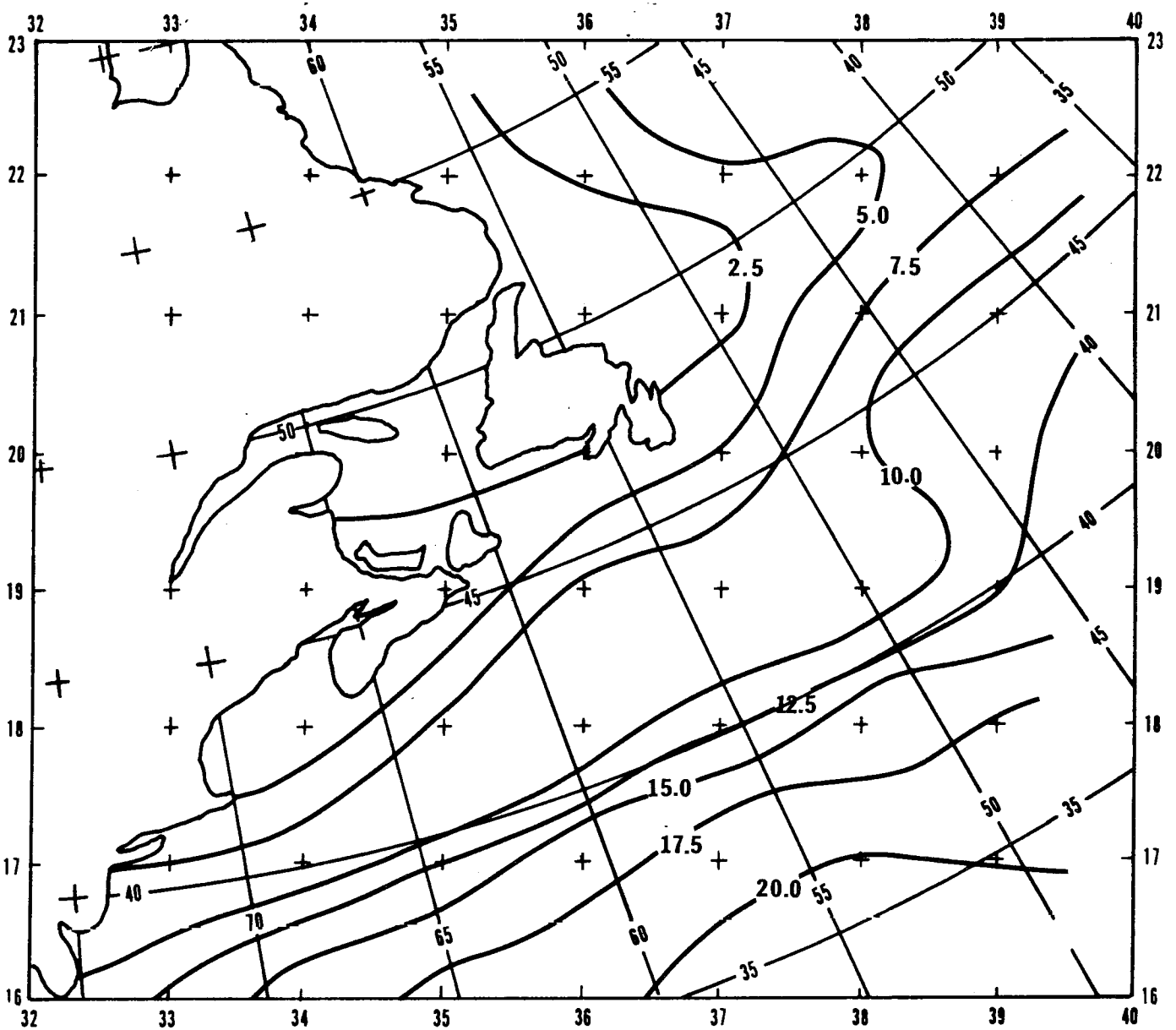

Figure 20. 10-day composite sea surface temperature (^{o}C) analysis from ship reports in Labrador Current-Gulf Stream boundary area 11 to 20 November 1968.

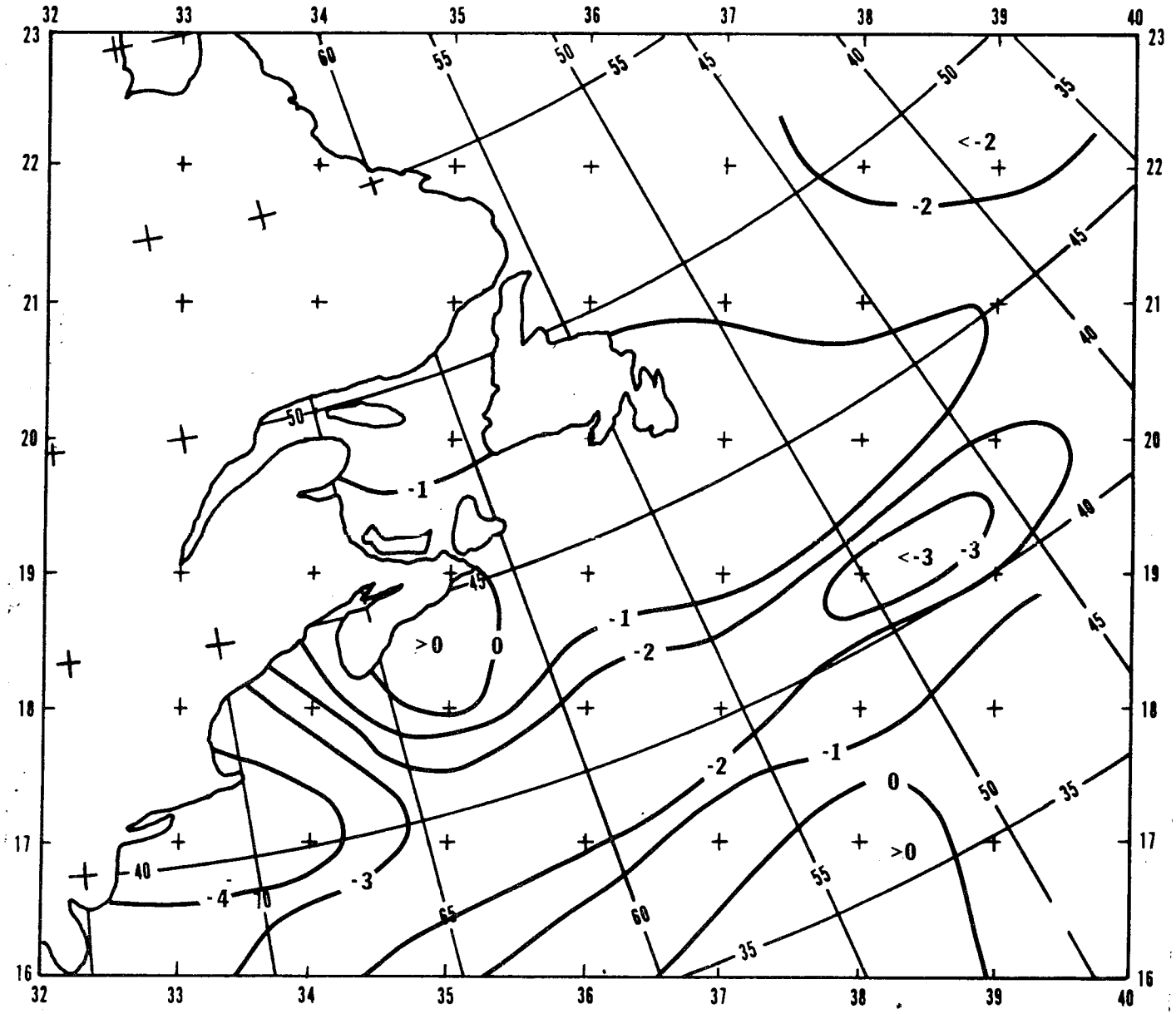

Figure 21. 10-day composite sea surface and surface air temperature difference analyses from ship reports in Labrador Current-Gulf Stream boundary area 11 to 20 November 1968.

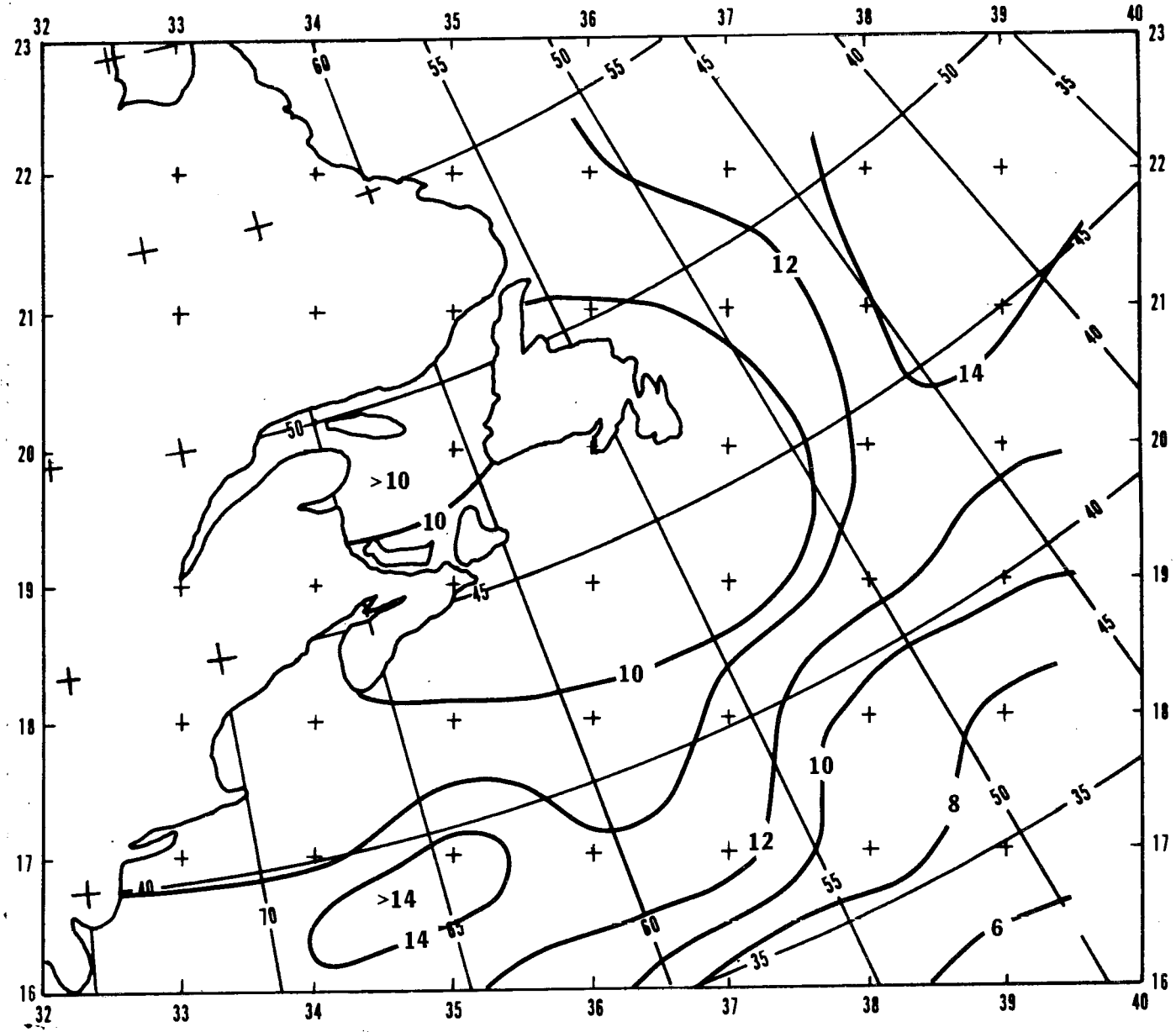

Figure 22. 10-day composite surface wind speed (m/sec) analysis from ship reports in Labrador Current-Gulf Stream boundary area 11 to 20 November 1968.

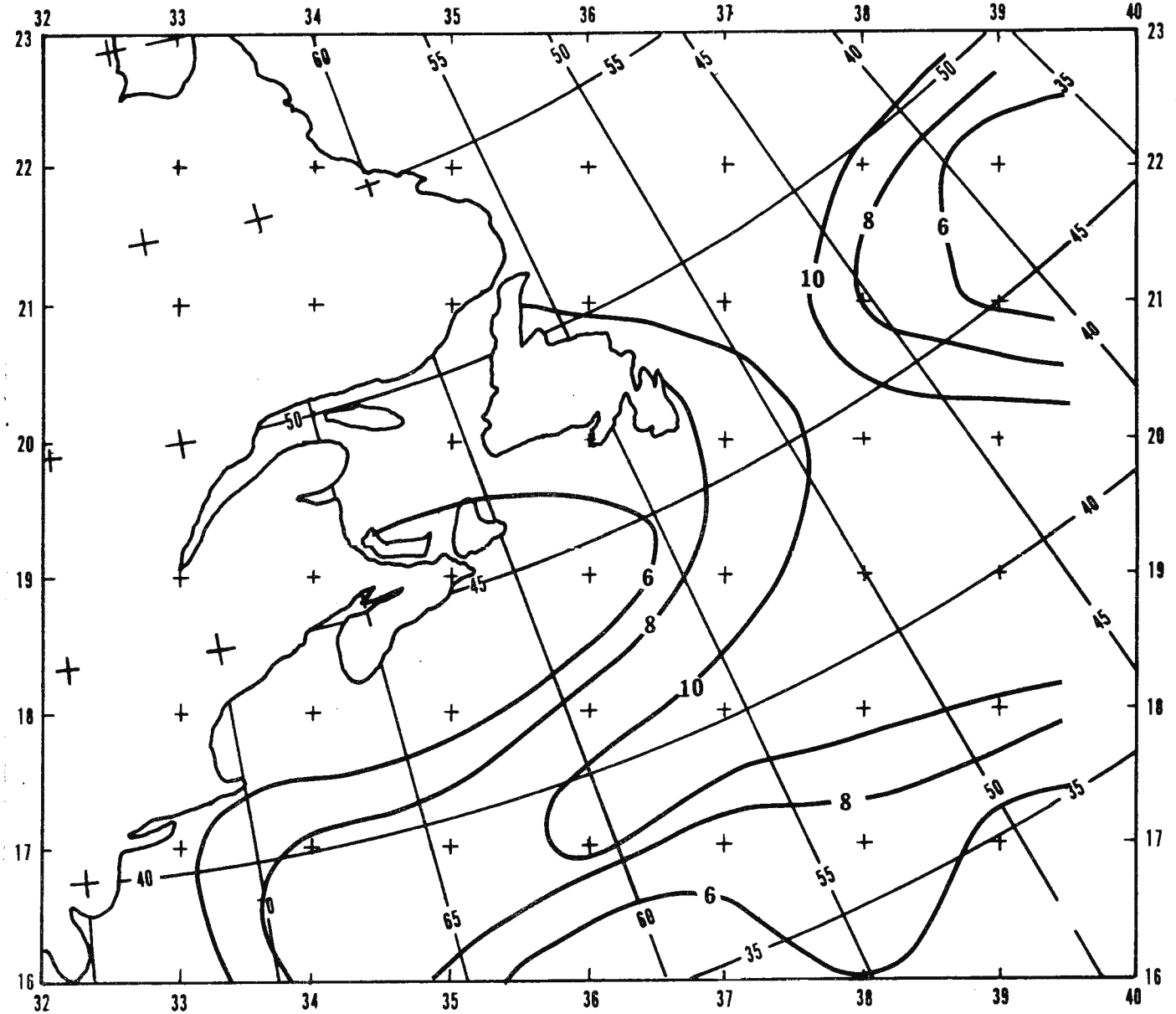

Figure 23. 10-day composite geostrophic wind speed (m/sec) analysis in Labrador Current-Gulf Stream boundary area 11 to 20 November 1968.